EFFECTS OF HYGROTHERMAL CONDITIONING ON EPOXY USED IN FRP COMPOSITES

By

B. PAIGE BLACKBURN

A THESIS PRESENTED TO THE GRADUATE SCHOOL
OF THE UNIVERSITY OF FLORIDA IN PARTIAL FULFILLMENT
OF THE REQUIREMENTS FOR THE DEGREE OF
MASTER OF SCIENCE

UNIVERSITY OF FLORIDA

2013

This thesis is dedicated to my parents, Margaret and Keith. Thank you for your constant love and support.

ACKNOWLEDGMENTS

I would like to thank the Air Force Academy Civil Engineering Department for granting me the opportunity to attend graduate school and pursue this research. My research advisor, Dr. Hamilton has been an excellent mentor throughout this experience. He has challenged me, sharpened my research approach and writing skills, and advanced my professional development. I would also like to thank Dr. Douglas and Dr. Ferraro for their guidance throughout this research and support in serving as my committee members. This research would have been more challenging without the hospitality of the Dr. Brennan research group in the materials science department who graciously shared their lab equipment and knowledge. In addition, I am appreciative of Gary Scheiffele, who provided instruction on guidance on FTIR testing. Finally I would like to thank my undergraduate summer intern, Grayson Lowman, for his work on my FTIR testing.

TABLE OF CONTENTS

page

LIST OF TABLES

LIST OF FIGURES

Abstract of Thesis Presented to the Graduate School
of the University of Florida in Partial Fulfillment of the
Requirements for the Degree of Master of Science

EFFECTS OF HYGROTHERMAL CONDITIONING ON EPOXY USED IN FRP COMPOSITES

By

B. Paige Blackburn

December 2013

Chair: H.R. Hamilton
Major: Civil Engineering

Fiber reinforced polymer (FRP) composites are installed on U.S. civil infrastructure to extend structure longevity. Durability of FRP composites is controlled by the adhesion of the composite to the structure surface, formed with epoxy. Epoxy is permeable to water and therefore is susceptible to negative effects of plasticization such as stiffness reduction when exposed to moisture. Heat, an additional threat to bond durability, will cause large reductions in both epoxy stiffness and strength if it exceeds the epoxy's glass transition temperature (Tg). Both effects can result in bond failure between the composite and the concrete surface. Some material specifications require testing of epoxy and the bonded interface following accelerated aging conditioning which includes exposure to moisture as well as temperatures up to 60°C.

Cold-cured epoxies used in carbon FRP composites, however, typically can have Tg values lower than 60ºC when cured under ambient conditions. Consequently, exposure to 60°C would result in a glass transition of the epoxy structure. Also, during exposure to elevated temperatures and water, the epoxy Tg itself can change. A Tg

reduced below the load testing environment and/or a plasticized matrix could skew load testing results by changing the mode of bond failure.

To understand how epoxy behaves in a bond application load test following conditioning, six FRP composite epoxies were monitored over time under varied hydrothermal conditions. Tg, conversion, and plasticization of the epoxy were measured with a DSC and FTIR at 2, 4, 8, and 12 weeks of exposure in either 60°C water, 30°C water, 60°C 100% RH, or 30°C 100% RH.

It was found that all epoxy types reached full saturation by 2 weeks of exposure and conversion values of 0.95 to 1.0 by 2 to 8 weeks. Tg of epoxies fluctuated by 5.5°C to 19.4°C. For every type of epoxy, 60°C immersion samples experienced the greatest Tg fluctuations. The highest Tg recorded during exposure was 68.1°C while the lowest recorded during exposure was 25.4°C.

CHAPTER 1
INTRODUCTION

Highway Bridge Deterioration

The American Society of Civil Engineers (ASCE) report card on U.S. infrastructure in 2013 found that 24.9% of bridges were either structurally deficient or functionally obsolete (ASCE 2013). Structurally deficient bridges were those determined to have critical load carrying elements that were in poor condition due to damage and/or deterioration, this included 1 of every 9 U.S. bridges. Structurally deficient bridges make up 1/3 of the total decking area in U.S., indicating that most of these are larger bridges in metropolitan areas. Functionally obsolete bridges were those that did not meet current standards, such as lacking required carrying capacities, or too narrow of lane widths. The report also found that the average age of U.S. bridges is 42 years old and that 30% of existing bridges have surpassed their original 50 year design life. The Federal Highway Administration (FHWA) predicts $20.5 billion needs to be spent annually by the U.S. to eliminate backlogs of required maintenance, repairs, rehabilitation, and replacements by 2028. Currently only $12.8 billion is spent annually on bridges.

Fiber Reinforced Polymer Composites

To address the problem of deteriorating bridges, cost and time efficient repair options are currently being explored. One solution that has gained popularity in recent years is to repair or strengthen bridges with fiber reinforced polymer (FRP) composites. While the use of these advanced materials is a relatively new phenomenon, American Association of State Highway and Transportation Officials (AASHTO) recently published design guidelines for the use of these materials to repair bridges (AASHTO LFRD

Bridge Design 2012). FRP composites are externally applied to load carrying bridge components to enhance their strength and serviceability. FRP composites apply additional reinforcement to structures expecting load increases, changes in functionality, or those that are deteriorated and are in need of repair. FRP composites are strongest in tension and therefore are applied to any structure that may need additional reinforcement in flexural bending, shear, concrete confinement or seismic strengthening.

There are two categories of FRP composites, carbon composites (CFRP) and glass composites (GFRP), with CFRP being the most prominently used in bridge repair. CFRP composites are typically formed using either a wet layup process or pre-cured laminates. Carbon fibers are solid, greatly elongated pieces of carbon material, with a length at least 100 times larger than their diameter (less than 1mm). These fibers are woven, knitted, or stitched into a carbon fiber fabric. This fabric is lightweight, flexible and can easily contour over smooth shaped concrete elements, excluding acute corners. FRP laminates are layers of fabric or mats that are bound in a cured resin matrix. Laminates can only be applied to flat surfaces unless cut (ACI Rep. No. 440.2R-08 2008).

Installation of FRP composites generally includes cleaning and sometimes roughening of the concrete surface, followed by surface saturation with an epoxy structural adhesive. Following surface preparation, wet layup FRP composites are also saturated in epoxy and then rolled onto the surface, while laminate FRP composites can be applied directly to adhesive. Some composites may include a final protective sealant

to conclude the FRP composite installation. In Figure 1-1, CFRP fabric is applied to the bottom flange of a bridge girder.

Figure 1-1. CFRP fabric installed around a bridge girder (photo courtesy of Dr. Trey Hamilton).

FRP wet layup and laminate systems have tensile strengths up to 550 and 380 ksi, respectively (ACI Rep. No. 440.2R-08 2008). But the strength of the repair is normally controlled by the epoxy bond between the concrete surface and the composite material. One concern is that over the life of the repair, environmental exposure could result in a weakening of adhesive bond strength. Laboratory testing has shown that epoxy bond strength decreases with exposure to environmental conditioning (El-Hacha et al. 2010; Stewart 2012; Tatar et al. 2013). Because epoxy bond integrity is crucial to FRP repair adequacy, understanding the effect of environmental exposure on the epoxy bond is paramount.

Accelerated aging techniques are implemented to assess FRP durability to environmental exposure over the service life of the structure (AASHTO LRFD Bridge Design 2012; ACI Rep. No. 440.2R-08 2008; ICC AC125 2012). Accelerated aging can involve any environmental factor that could cause degradation. Factors that typically cause FRP materials to deteriorate include moisture, alkali, UV radiation, abrasion/impact and elevated temperatures (ACI Rep. No. 440-07 2007). One example

is hygrothermal conditioning, where samples are exposed to moisture and elevated temperatures simultaneously.

A concern with accelerated aging is that some exposure testing as required in the AASHTO FRP composite guidance and in the International Code Council (ICC) FRP acceptance criteria call for high temperatures, up to 60ºC. These specifications are presented in Chapter 3. Concern for including elevated temperatures during exposure exists because previous research has demonstrated significant alterations in epoxy behavior to result (Stewart 2012; Moussa et al. 2011). This research investigates how epoxy characteristics change during hygrothermal exposure with elevated temperatures.

CHAPTER 2
LITERATURE REVIEW

Epoxy

Structural epoxy is available as a resin or as a paste. Both result from the mixture of two components. Typically, part A for resin epoxy has the consistency of molasses or honey, while part A for paste epoxy contains sand particles and is more viscous. Part A makes up the epoxy body for both types. It is generally based on bisphenol A molecules hosting an epoxide functional group at both ends as pictured in Figure 2-1A, forming the monomer in the epoxy structure (Stewart 2012). The hardener, Part B, is composed of amines that react with the epoxide groups to form covalent bonds (Figure 2-1B). The amines bond the monomers together in a linear fashion to form polymer chains (Figure 2-1C). The amines also cross-link the polymer chains together through more covalent bonds as depicted in Figure 2-2 (bisphenol A not imaged). This process is the curing of the epoxy and with subsequent cross-linking a non-crystalline hardened molecular structure is formed (Douglas 2013).

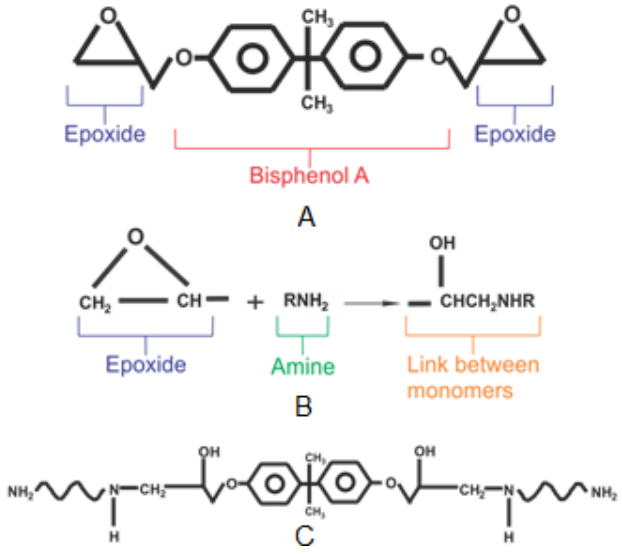

Figure 2-1. Epoxy Chemistry. A) Part A molecules. B) Reaction between epoxide and amine. C) Linear formation of polymers.

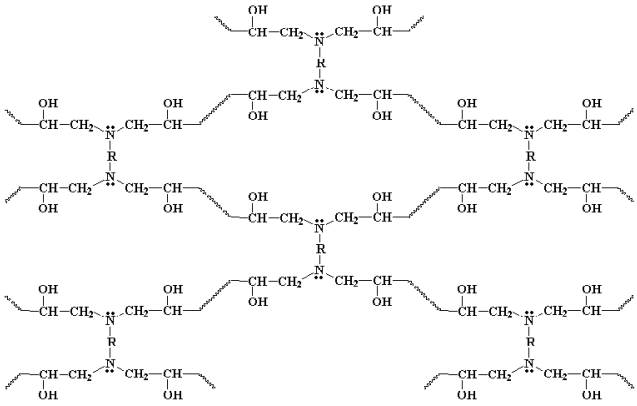

Figure 2-2. Cross-linking of polymer chains (bisphenol A molecules not imaged).

Assuming that parts A and B are proportioned and mixed correctly, and that adequate temperature and time are provided (varies by epoxy type), the epoxy will reach a maximum amount of cross-linking, referred to as 100% cure. Conversion values are utilized to compare epoxies with different degrees of cure and has a scale of 0 to 1.0. For example a fully cured specimen has a conversion of 1.0, a zero cured sample has a conversion of 0.0, and partially cured sample lies somewhere between 0 and 1.0. The higher the density of cross-linking between polymer chains, then the higher the conversion (Choi 2011). Once cured, the epoxy molecules are frozen in place similar to glass. In this glassy state the epoxy has high levels of both stiffness and strength, making it a useful product for structural repairs.

When applied to a surface, the epoxy adheres both mechanically and chemically. While the exact nature of the chemical bond is not known, it is thought to consist of mostly hydrogen bonding between surface molecules. Epoxy bond strength is thought to be due primarily to mechanical bonding via epoxy and concrete interlocking (Djouani et al. 2011; Kim et al. 2010; Stewart 2011; Tatar et al. 2013).

Mechanical interlock is formed when liquid epoxy fills the irregular shape of the roughened concrete surface (Kim et al. 2010). As the epoxy hardens inside these surface pores, a mechanical interlock is formed as illustrated in Figure 2-3A. Once cured, the epoxy has high structural stiffness (around 2.5 x 10^5 psi (1,724 MPa) for epoxies studied here), giving it capability to transfer high loads between the concrete and FRP composite. As long as the epoxy maintains stiffness, the integrity of the mechanical interlock will be preserved. Unfortunately, the epoxy stiffness may be susceptible to change under certain environmental exposures.

Unlike most materials, amorphous (non-crystalline) polymers, such as epoxy, lack a melting point transforming them from a liquid to a solid state. Rather, they have a glass transition temperature (Tg) transitioning them from a glassy state to a rubbery state. Epoxy strength and stiffness decrease following transition from a glassy state to a rubbery state (Aiello 2002; Douglas 2013; Stewart 2012). Take a more common polymer, a slice cheese for example. When chilled the cheese is in a glassy state; it holds its form and is relatively firm. When heated the cheese reaches Tg, losing its firmness, allowing it to flow. The cheese has not melted to a liquid state, but rather has transitioned into a rubbery state, which is more viscous than a liquid, but is . This same behavior occurs when heating cured epoxy. Epoxy with a temperature below Tg is in a glassy state, which means that the covalent bonds between polymer chains are unable to rotate and are “frozen” in place. Once the Tg is exceeded, however, the covalent bonds are capable of rotating, but remain intact. Therefore, the general shape of the epoxy during the glassy state is maintained, but its stiffness and strength are reduced.

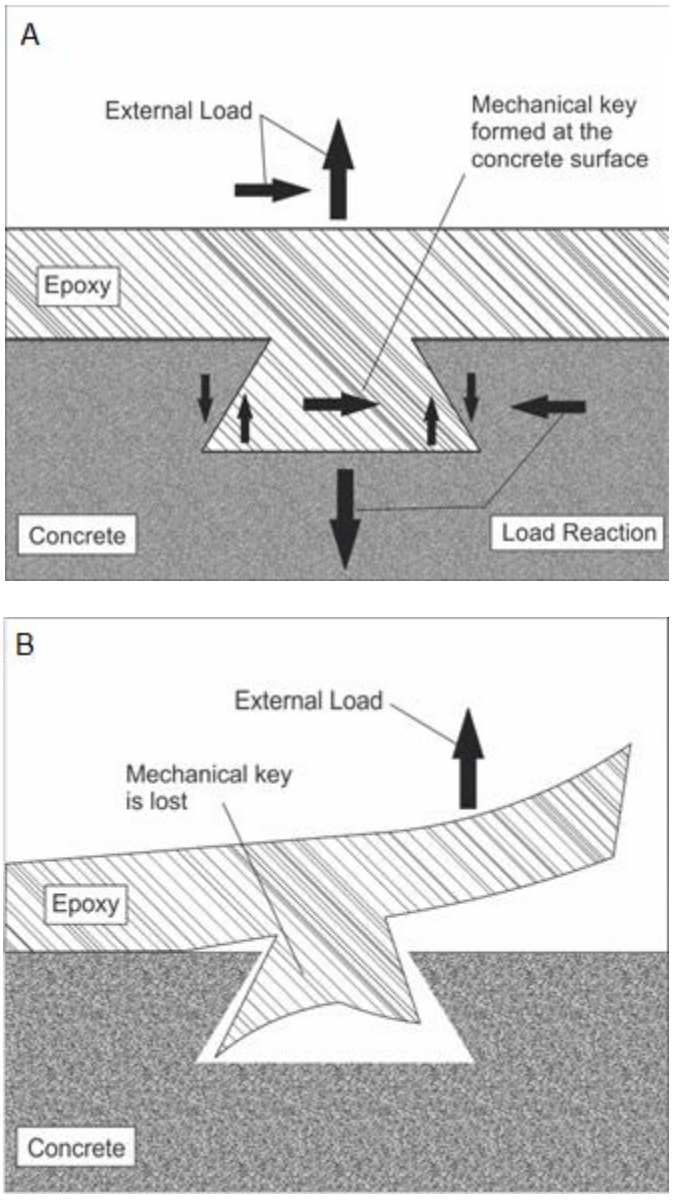

Figure 2-3. Mechanical bonding between hardened epoxy and concrete surface. A) Original mechanical interlock provided in a glassy state. B) Loss of mechanical interlock between epoxy and concrete caused by a lack of epoxy stiffness in the rubbery state.

The value of epoxy Tg is dependent on polymer chain mobility. The easier it is for the polymer chains to move, the lower Tg will be (Douglas 2013; Frigione 2006). Essentially, the less rigid the epoxy molecular structure, the less thermal energy is required for transition from a glassy state to a rubbery state. Amounts of free volume

and cross-linking (measured by conversion) effect polymer chain mobility and consequently change the epoxy Tg.

Cross-linking restrains polymer chain mobility by interconnecting individual chains together. Therefore, the more cross-linking or covalent bonding, the less chain mobility and the larger Tg. Covalent bonding between polymer chains increases as the epoxy cures, but under room temperature conditions for two or more weeks, most structural epoxies range from a conversion of 0.8 to 1.0, which means that 80-100% of possible covalent bonds were formed (for most epoxies). Exposure to temperatures above those experienced during initially curing cause additional cross-linking. Depending on the temperature and length of exposure, epoxy can increase from the room temperature conversion to 1.0, (Choi 2011). Any elevated temperature treatment above initial cure conditions that increase cross-link density is called added cure. Samples that have experienced added cure require more thermal energy to transition into a rubbery state than those without added cure, and consequently have a larger Tg (Choi 2011; Frigione 2006).

Chain mobility is also affected by the amount free volume in the polymer structure. Free volume is the available space within the polymer chain network on a microscopic level (Douglas 2013; Frigione 2006). The more free volume between polymer chains, the more space they have to move around, hence less thermal energy is required to convert the epoxy into a rubbery state. Water absorption can lead to increases in free volume in the epoxy. The sides of polymer chains are lined with hydroxyl groups, as illustrated in Figure 2-2. When exposed to moisture, water molecules are drawn into the epoxy and react with hydroxyl groups via hydrogen

bonding (Fridgione 2006; Choi 2011). This hydrogen bonding creates more space in between the cross-linked polymer chains, thereby enlarging the free volume available. Water absorption into the epoxy is referred to as plasticization and will cause decreases in Tg (Fridgione 2006; Stewart 2012; Choi 2011).

Added cure and plasticization can be described by considering a plate of spaghetti, where the polymer chains are represented by the noodles. When the spaghetti is hot and fresh the noodles slide around easily, representing a rubbery state. Epoxy in a glassy state is similar to spaghetti that has been left on the kitchen counter for a couple days, becoming a hard brick with noodles that are stuck together. Added cure is comparable to leaving spaghetti out even longer, becoming harder and more rigid. With harder spaghetti the microwave time increases in order to loosen the spaghetti back up, analogous to added cure increasing the Tg. To reduce the hardness of old spaghetti water could be sprinkled to loosen up the noodles, decreasing the microwave time. Plasticization has an analogous effect on epoxy, decreasing Tg.

Tg Measurement

Several techniques exist to calculate the Tg of polymers. There is no particular standard method preferred amongst researchers; each method provides acceptable data. Glass transition occurs over a temperature region and each method chooses a different temperature within the region to indicate the transition. This disparity in calculation can produce a Tg that is up to 25°C different from another approach. No conversion of Tg values between methods is officially exercised, therefore knowledge of what method a given Tg value was calculated from is important. Manufacturers, engineering design codes, and researchers all employ different test methods for Tg, therefore a description of each technique is paramount.

Dynamic Mechanical Analysis (DMA)

DMA testing requires a small bar shaped epoxy sample roughly 1-4mm thick, 5mm, and 20mm long. The DMA applies cyclic midpoint loading to the bar sample in a temperature controlled chamber normally heated at 5°C per minute. The sample's response to stress, temperature, and load frequency is measured. By measuring deformation of the sample during the applied stress a storage modulus, E`, is calculated, measuring the sample's elastic behavior. Also calculated is damping, represented by tan($\delta$), and is a measurement of the sinusoidal phase shift between cyclically applied stress, and the cyclic strain response. As the DMA chamber temperature reaches close to Tg, both E` and tan(δ) indicate the transition from a glassy state to a rubbery state as the epoxy stiffness reduces.

To calculate Tg, either E` or tan(δ) can be plotted against temperature to create a curve (Figure 2-4). Different industries use different points along these curves to represent Tg. The most common points include the onset of storage modulus step change, the peak tan(δ), and the peak of the storage modulus derivative as Figure 2-4 details. Even when looking at solely DMA data, the Tg can be up to 15°C different when its calculated at point 1 in Figure 2-4 compared to calculation at point 2. Both Tg values would be considered acceptable as long as the point of calculation was properly documented. ASTM D4065 (required by ICC) details operation of the DMA but does not indicate which point should be taken as the Tg. ASTM E1640 (required by AASHTO), takes point 3 of Figure 2-4 to be the Tg.

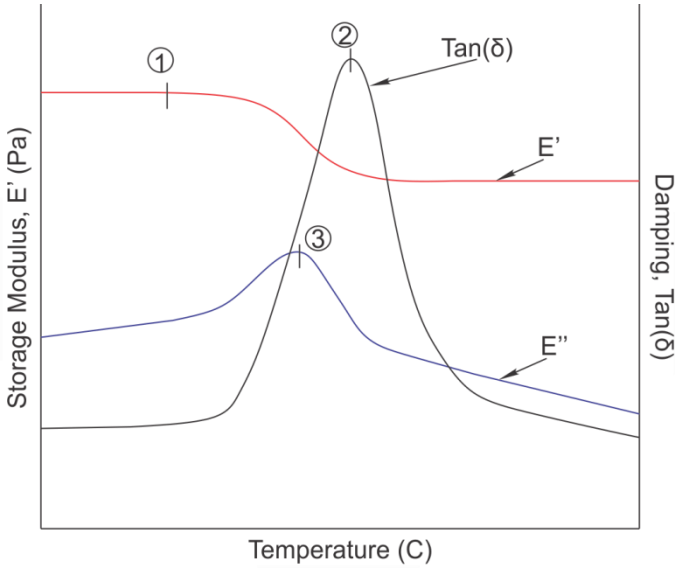

Figure 2-4. DMA Tg calculation. 1) Tg at E' onset. 2) Tg at tan(δ) peak. 3) Tg at E'' peak.

Thermo-mechanical Analysis (TMA)

The TMA has a similar test set up at the DMA, but instead of a dynamic load, a static load is applied. A probe provides a very small constant force onto a cylindrical sample as a temperature controlled chamber is slowly heated. The probe can move vertically and is connected to a linear variable differential transformer (LVDT) that measures linear displacement. As temperature increases, the free volume inside the sample will expand, physically pushing against the probe, and displacing it vertically. Change in probe height is recorded and plotted against increasing temperature, the rate at which the height changes is the coefficient of thermal expansion (CTE) and the slope of the TMA curve.

Once the glass transition region is reached during heating, the CTE increases indicating the free volume expansion created during transition from a glassy state to a rubbery state. Tg is then taken at the change in CTE. An example of a TMA curve is

presented in Figure 2-5, note that Tg is located at the intersection of the two slope extrapolations. Testing epoxy in the TMA for Tg is detailed in ASTM E831.

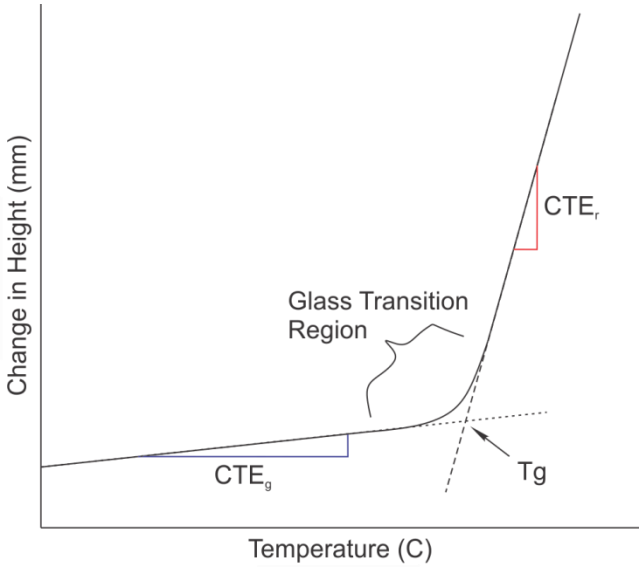

Figure 2-5. TMA Tg calculation. Where CTE_g is the CTE of a glassy state, and CTE_r is the CTE of a rubbery state.

Differential Scanning Calorimeter (DSC)

The DSC unlike the TMA and DMA, does not apply loading to the specimen. Rather than measuring mechanical properties such as modulus and deflection, the DSC measures heat flow. An epoxy sample and a reference sample rest on a two separate temperature detecting posts in a temperature controlled chamber (Figure 4-3). The DSC increases the temperature of each sample a rate of 10°C per minute and measures the heat flow into each sample required to maintain that temperature increase.

This measurement is directly related to specific heat capacity, which is the energy required to increase a material by one degree. The heat flow into the epoxy sample is subtracted from the heat flow into the reference and heat flow difference is plotted verses temperature creating the DSC curve. During glass transition, epoxy heat capacity increases, resulting in a step change in the DSC curve which represents the

glass transitions region (Figure 4-4B). DSC theory and operation per ASTM 1356-08 are detailed further in Chapter 5.

Heat Deflection

Heat deflection tests are not designed to calculate Tg, but are exercised by some epoxy manufacturers in lieu of traditional Tg testing. Heat deflection testing applies a static load of 264 psi to an epoxy bar sample and measures the displacement of the loading mechanism into the sample. The temperature of the epoxy is slowly increased until a deflection of 0.25mm is reached. The temperature at which 0.25mm is reached is recorded as the heat deflection temperature (HDT) according to ASTM D648. The HDT is a similar temperature value to Tg, and indirectly indicates the occurrence of glass transition.

Because glass transition occurs over a temperature region and the DMA, TMA, DSC, and HDT all measure Tg through different processes it's not surprising that varied Tg values could be reported for one material. Normally the Tg variability is only 5 to 10°C between methods but can be as much as 25°C, for example between the DSC and the DMA (if Tg is measured at the tan(δ) peak). When testing epoxy for Tg with any thermal analysis equipment it is vital to calculate the Tg from the first heat cycle if multiple cycles are used. Heat cycles, for example -20ºC to 120ºC is appropriate for most epoxies, will cure the epoxy. Therefore, if multiple cycles are conducted, the Tg from any additional cycle beyond the first will reflect the Tg of fully cured epoxy which will be higher than that of the original specimen prior to testing. Previous research studied this phenomenon with the DMA and found up 30ºC differences in Tg values

calculated from different heat cycles, illustrating the importance of calculating Tg from the first heat cycle conducted (Jaipuriar et al. 2011).

FRP Composite Testing

Currently, industry testing standards (AASHTO LRFD Bridge Design Requirements 2010, ACI 2007, ICC 2012) require that the durability of FRP composite bond be tested by direct tension pull-off (ASTM D4541), which is also used for quality control in the field. The direct tension pull-off test results in mode I fracture behavior (pure separation between FRP composite and concrete due to tension). Research has been conducted that suggests the use of a small beam test so that the mode II fracture behavior (slip between FRP composite and concrete surface during bending) is captured when conducting durability testing (Dolan 2008, Gartner 2007, Tatar 2013).

The concrete beam specimens are 14 inches (35.5 cm) long with a 4 inch by 4 inch (10.2 cm x 10.2cm) square cross section (Figure 2-6). Each beam receives a 1/8 inch (3.2mm) wide saw cut, 2 inches (5.1 cm) deep into the beam, across the 4 inch (10.2 cm) beam width. The saw cut notch is then repaired with an FRP composite. Six FRP composite systems from six different commercial manufactures are tested. Each FRP composite repair consists of a 1 inch by 8 inch (25mm x 203mm) piece of CFRP fabric or laminate laid perpendicular to the saw cut notch. The CFRP composite is applied following the manufacturers specifications.

Beams are then either immersed in water or placed in 100% humidity conditions at an elevated temperature in the range of 30°C to 60°C for 1, 2, or 8 weeks. Beams are tested in a 3 point bending test, as pictured in Figure 2-7, within 24 hours after removal from exposure. The strength results and failure mode of the exposed beams are compared to that of the control beams.

The beam project utilizes 60°C (140°F) for some exposure conditions; similar to current AASHTO and ICC testing standards (detailed in Table 2-1 and Table 2-2). It has been argued that temperatures this high may exceed epoxy Tg, thereby reducing the strength and stiffness of epoxies used in FRP composites. Therefore, the concern is that the results from beams exposed to 60°C will fail at much lower loads and perhaps in a different failure mode, and could not be fairly compared to beams not exposed to 60°C.

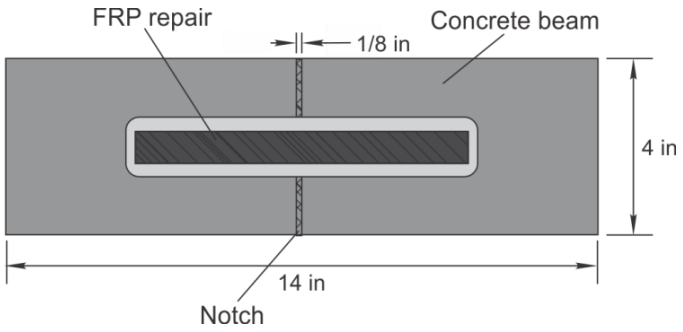

Figure 2-6. Plan view of FRP repair on miniature concrete beam.

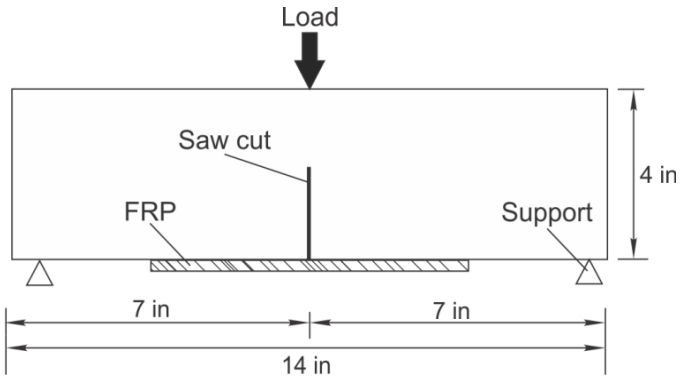

Figure 2-7. FRP beam 3 point bending test.

Interface Failure Modes

When FRP composite repairs are tested there are five locations where failure can occur as labeled in Figure 2-8, 1) In the FRP composite layer, 2) At the interface between the FRP composite and the epoxy, 3) In the epoxy layer, 4) At the interface

between the epoxy and the concrete, 5) In the concrete layer (Gartner 2007; Quiao 2008).

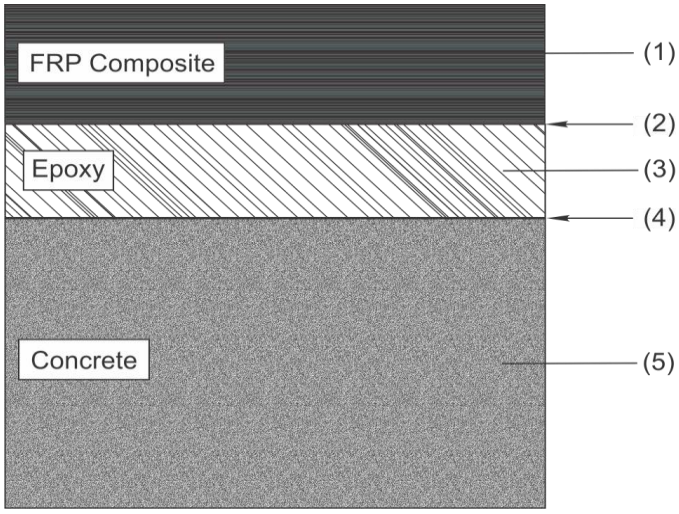

Figure 2-8. Cross section of an FRP composite illustrating locations of different failure modes.

The most desired failure is a cohesive failure at location four in Figure 2-8, where concrete paste and aggregate just below the epoxy bond rupture (Figure 2-9). A cohesive failure demonstrates the epoxy bond is stronger than concrete itself. Consequently, during tensile or flexural loading the interlock mechanisms (depicted in Figure 2-3A) are sustained and rupture away from the concrete surface. This is the assumed failure mode for FRP repair design (ACI 2007).

A less desirable failure mode is an adhesive failure, where delamination occurs directly in between the epoxy and concrete layers. In an adhesive failure, mechanical interlock is completely lost as Figure 2-10 demonstrates (similar to Figure 2-3B). Hence, the FRP composite strip comes off clean and the concrete surface remains smooth. Adhesive failures demonstrate the epoxy concrete bond as the weakest element of the FRP composite repair for that particular test. Also frequent is a mixed mode failure when elements of both adhesive and cohesive failures appear (Figure 2-11).

To avoid adhesive failures, the integrity of the mechanical interlock between the epoxy and concrete must be preserved. Mechanical interlock quality is provided by both the longevity of high epoxy stiffness and a strong yet porous concrete surface. Therefore, epoxy behavior and bond integrity are directly related and determine the success or failure of an FRP composite repair.

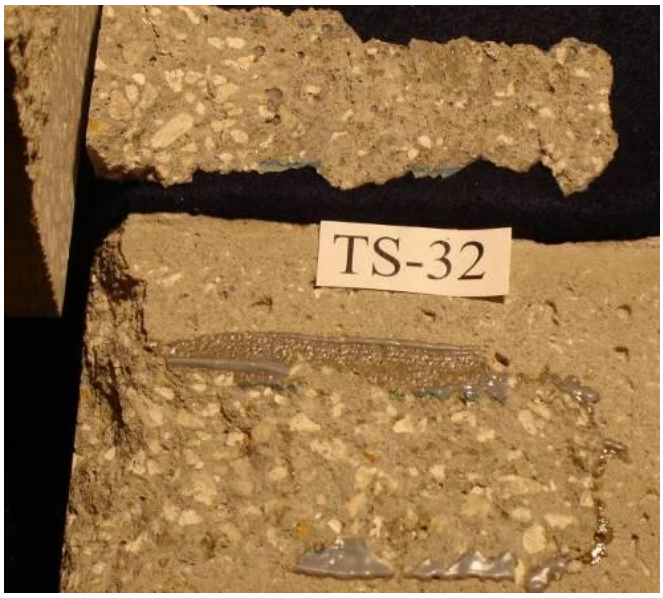

Figure 2-9. Cohesive failure at epoxy/concrete interface (Gartner 2007).

Figure 2-10. Adhesive failure at epoxy/concrete interface (Gartner 2007).

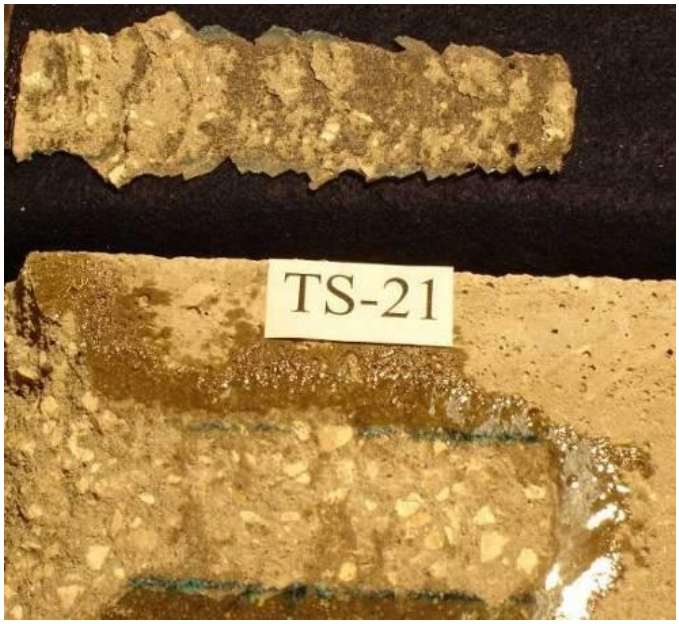

Figure 2-11. Combination of both adhesive and cohesive failure behavior (Gartner 2007).

Standards for FRP Composite Durability

Although concrete repair with FRP composites is relatively new compared to other methods, materials testing standards have been developed to ensure FRP composite durability. The early stage of the design requirements provides interesting comparisons to independent research testing. Testing requirements of FRP composite bond quality to concrete and epoxy are reviewed. Requirements for individual FRP fabrics, laminates and composites exist but not detailed here.

ICC Acceptance Criteria

The International Code Council (ICC) provides acceptance criteria for concrete strengthening using externally bonded FRP composites (AC125 2012). AC125 requires FRP composite and concrete bonded samples to be formed and tested according to ASTM D4541, a traditional tensile pull off test, or to ASTM C297, where a tensile pull off test is performed on an FRP composite bonded in between two concrete surfaces. Bond

samples must have a tensile strength of at least 200 psi following exposure according to conditions A-E, listed in Table 2-1, and fail cohesively through the concrete substrate.

Epoxy specimens are formed and tested according to ASTM D4065 or ASTM E831. These standards use DMA and TMA respectively, both call for epoxy bar samples that are approximately 1-4 mm thick x 5 mm wide x 5-20 mm long and test for Tg. AC125 requires a minimum Tg of 60°C for control specimens and for those exposed according to all of Table 2-1.

Table 2-1. ICC exposure conditions.

Environmental Durability Test	Relevant Specifications	Test Conditions	Test Duration (hours)	Percent Retention* 1,000 hrs	3,000 hrs
A) Water	ASTM D2247 ASTM E104	100%RH, 38°C	1,000, 3,000, 10,000	90	85
B) Saltwater	ASTM D1141 ASTM C581	Immersion, 23°C	1,000, 3,000, 10,000		
C) Alkali	ASTM C581	Immersion in CaCO3, pH=9.5, 23°C	1,000 and 3,000		
D) Dry heat	ASTM D3045	60°C	1,000 and 3,000		
E) Freeze – Thaw	N/A	20+ cycles: 4 hrs at -18°C, 12+ hrs at 38°C and 100%RH	500	90	
F) Fuel Resistance	ASTM C581	Immersion in diesel fuel reagent	4+	N/A	

* Some conditions require exposed samples to retain a percentage of the equivalent control sample value.

AASHTO Design Standard

American Association of State Highway Transportation Officials (AASHTO) provides strength and durability requirements for FRP composites applied to highway structures (AASHTO LRFD Bridge Design Requirements 2010). According to the 2012 AASHTO bridge committee, contractors are required to submit evidence of acceptable

quality control procedures conducted by the manufacturer of the FRP composite. Bond samples (form not specified) following exposure according to Table 2-2, must maintain a bond strength of at least 200 psi or $0.65 \cdot \sqrt{f`c}$, whichever is greater. Where $f`c$ is the specified concrete compressive strength. A strength test method is not specified and is left to be determined by the engineer of record.

Epoxy samples are formed and tested according to ASTM E1640. This standard also uses the DMA to acquire epoxy Tg and requires small bar sized samples. Following exposure listed in Table 2-2, the Tg must retain no less than 85% value of the control Tg and remain at least 22°C above the maximum design temperature as defined in article 3.12.2.2 of AASHTO LRFD 2010.

Table 2-2. AASHTO exposure conditions.

Environmental Durability Test	Relevant Specifications	Test Conditions	Test Duration (hours)
A) Water Immersion	Not specified	38°C, distilled	1,000, 3,000, 10,000
B) UV and Humidity	ASTM G154	8hrs UV at 60°C, 4hrs condensation at 50°C	12
C) Alkali Immersion	Not specified	Immersion in CaOH2, pH=11, 23°C	1,000, 3,000, 10,000
D) Freeze Thaw	ASTM C666	100 cycles	Not specified

ACI Design Guide

The American Concrete Institute (ACI) does issue distinct requirements for FRP composites bond strength and durability but does provide recommendations for their use in the ACI 440.2R committee report. The report does not suggest any prior materials testing besides those conducted at the construction site. For bond critical applications, the report suggests to core concrete samples from the structure to perform tension pull off tests according to ASTM D4541. Samples are recommended to exhibit

bond strength of at least 200 psi and fail adhesively through the concrete substrate. No sample conditioning is mentioned in the report.

Epoxy Tg is suggested to be at least 15°C higher that the service temperature of the FRP composite in dry environments. No recommendations are provided for Tg in non-dry environments. The report calls for more research to be conducted in FRP composite behavior following extended exposure to moist environments.

Review of Previous Research

Because FRP composites are relatively new in the construction and repair industry, little is known about their durability under environmental conditions. Prior research has isolated how different exposure conditions effect epoxy Tg, strength and stiffness. This research intends to extrapolate the data from prior research to provide more insight on epoxy durability to the FRP composite field.

Moussa et al. (2011) investigated how Sikadur 30, a two part commercial paste epoxy reacted following exposure to a range of temperatures; -35º to 150º C. The manufacturer reported a fully cured Tg of 62º C (resulting from DMA). After two weeks of curing under ambient conditions Moussa et al. reported a DSC calculated Tg of 45º C for epoxy samples prior to exposure. Two exposure categories were explored. The first explored the relationship between temperature and strength, testing samples after 30 minutes of exposure to either -35, 0, 20, 30, 40, 50, or 60ºC. After 30 minutes tensile experiments were conducted in a climate controlled chamber where samples maintained their respective exposure temperature. Moussa et al. found that between -35º and 60º C sample stiffness and strength reduced from 14.1 GPa and 49.4 MPa to 0.16 GPa and 5.27 MPa respectively, proving a strong relationship between mechanical performance and temperature (Figure 2-12).

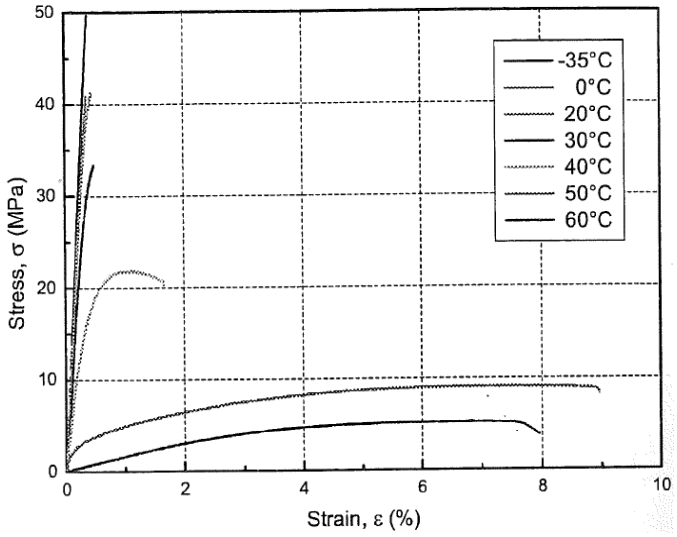

Figure 2-12. Typical stress-strain curves of specimens exposed to temperatures between -35 and 60°C (Moussa et al. 2011).

The second exposure series investigated effects of varied exposure periods on strength, testing 40º and 50º C samples, conditioned for either 30 minutes, 2 hours, or 4 hours. Samples exposed to 40º C exhibited a constant stiffness, independent of exposure length, because the exposure temperature was below the Tg (45º C). Conversely, 50º C samples (exposed above the Tg) initially experienced a large drop in stiffness after 30 minutes of exposure, but added cure beyond 30 minutes of exposure created a complete stiffness recovery. The elevated temperature increased the Tg from 45º C above the 50ºC exposure by increasing cross-link density. Between 30 minutes and 2 hours of exposure the stiffness properties dramatically changed illustrating the dependency of mechanical properties on exposure length (see Figure 2-13).

Strength recovery was studied in the third exposure series. Samples were exposed to 60, 100, or 150º C for 30 minutes and then allowed to cool to 20, 40, 50, or 60º C prior to tensile tests. Specimens cooled to 60°C exhibited nearly zero stiffness during tensile tests, but with cooler test temperatures, specimens displayed improved

stiffness. All specimens cooled to 20º C, regained complete stiffness properties of the glassy state. Samples conditioned under 100 and 150°C had improved stiffness, greater than that of 60°C and control samples due to added cure. Figure 2-14 exemplifies that temperatures above Tg do not alter the stiffness of the epoxy once sufficiently cooled, but actually improve it.

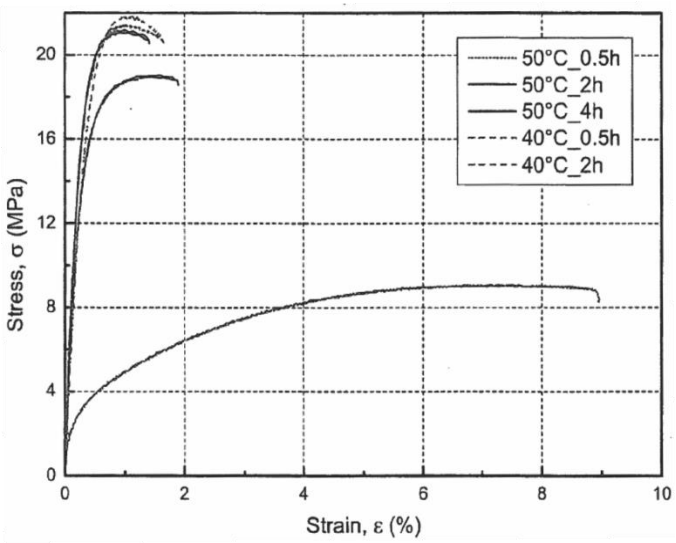

Figure 2-13. Typical stress-stain curves for different time periods within the glass transition range (Moussa et al. 2011).

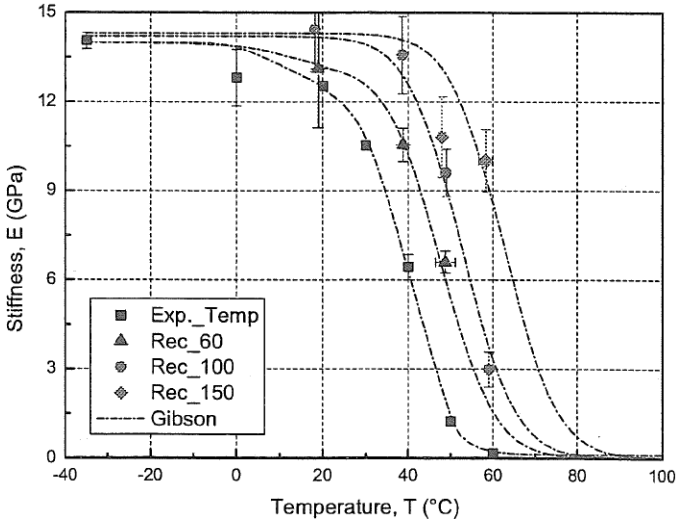

Figure 2-14. Recovery behavior and effect of post-curing temperature on stiffness (exposure duration of 30 minutes) (Moussa et al. 2011).

Stewart (2012) investigated epoxy mechanical response to UV radiation and hygrothermal (water and heat combination) conditioning. One model epoxy and one commercial epoxy were exposed to water temperatures ranging from 30º to 90ºC (hygrothermal exposure). Both epoxy types were also conditioned under a UV irradiance of 0.68 W/m^2, 60º C, and 45% humidity and either with or without water spray. Samples were exposed for up to 8 weeks, and were tested every 2 weeks. Tensile tests and measurements of sample cross sectional area were conducted.

Following 8 weeks of hygrothermal exposure, Stewart found that up to 33% of the modulus and 38% of the peak tensile strength was lost. Stiffness and strength proved to decrease with increased temperature of exposure, with 90°C exposure producing in the lowest strength values. The ultimate strain increased from 3.5% up to 5.1%. All samples showed an increase in cross sectional area, up to 7.47% enlargement. Reduction of strength and stiffness was attributed to absorption of water molecules via hydrogen bonding with epoxy hydroxyl groups as noted by previous research and literature, this process is also known as plasticization (Lu et al. 2001 and Nunez et al. 1999). During tensile testing, not only did samples have reduced moduli and strength, but they also exhibited necking, unlike control samples which had no necking and failed in a brittle manner.

Samples exposed to UV either with or without water spray did not have as large of a decrease in stiffness and strength as water alone. All UV samples did have a slightly lower modulus compared to the control, but the peak stress of UV samples was variable, and no consistent behavior was determined. Ultimate strain appeared to decrease by the eighth week of exposure, but it was not statistically significant. Stewart

believed that the effects of UV degradation and water absorption were in competition with each other, making results difficult to explain.

Choi (2011) measured changes in epoxy Tg due to hygrothermal exposure from 1 to 28 days of water immersion under temperatures that ranged from 30º C to 60º C. Two commercial epoxies and one ideal or “model” epoxy were tested. The model epoxy was a clear two-part resin epoxy composed of diglycidyl ether of bisphenol A (DGEBA) and poly(oxypropylene) diamine (POPDA, Jeffamine D-230), manufactured by Huntsman. Epoxy samples were cured in ambient conditions for 4 weeks and then exposed for 1, 2, 4, 7, 14, or 28 days in 30º, 40º, 50º, or 60º C water.

Following exposure a DSC was utilized to measure Tg. Samples were also tested in the fourier transform infrared spectrometry (FTIR; Nicolet Magna 760, Thermo Electron Cooperation) with a CaF2 beam splitter and an MCT detector in order to track how increased cross-link density and plasticization affected the Tg. The DSC and FTIR provided Tg, conversion and relative amount of water absorbed for each sample. With these data the individual effects of cross-link density and plasticization on Tg were isolated.

With the FTIR, it was found that epoxy samples increased in water content by 200-300% from prior to exposure. This increase occurred during the first 4 days of exposure, but beyond 4 days, water content remained at a constant level for all temperatures. During the first few days, samples under higher temperatures absorbed more water due to an increase in water diffusion. But over time the amount of water absorbed converged to the same value despite exposure temperature. By tracking the

amount of water absorbed losses in Tg were correlated with plasticization of the epoxy molecular structure.

Elevated temperatures during exposure caused increases in cross-link density. Cross-linking reduced polymer chain mobility and thereby increased the Tg. Samples started around 0.80-0.88 conversion (varied by epoxy type) after curing in ambient conditions for 4 weeks. FTIR results showed that samples exposed in 60º C water were nearly at 1.0 conversion after one day of exposure. Lower exposure temperatures did not increase sample conversion as quickly, which did not plateau until about 2 weeks into exposure. Higher temperatures plateaued at larger conversions. For instance, samples immersed in 50º C water reached 0.97-1.0 (based on epoxy type), 40º C samples up to 0.94-0.97, 30º C samples up to 0.91-0.95, and control samples only increased by 0.01 over a 28 day exposure period.

DSC test results exhibited Tg values that both increased and decreased over the 28 day period, as depicted in Figure 2-15. Choi suggested that the effects of plasticization and cross-linking were in competition with each other and at certain stages of exposure, one would have more effect than the other. Following 2 weeks of exposure the Tg plateaued for all three types of epoxy tested. By 28 days, epoxies A and B reached a Tg larger than the respective control. Total increases for A and B epoxies ranged from +1º C to +14ºC based on the epoxy type and temperature of exposure. Epoxy C samples demonstrated less change in Tg but plateaued to +/- 5º of the control Tg based on the exposure temperature.

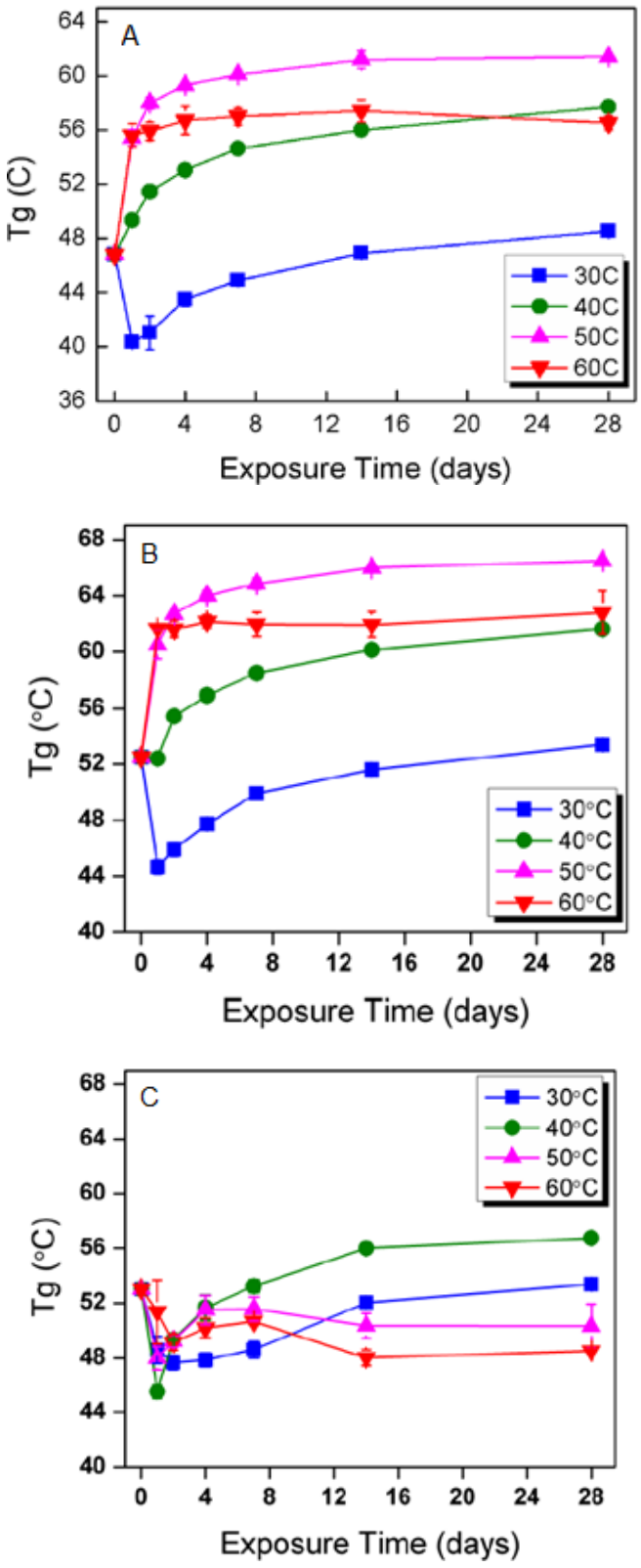

Figure 2-15. Variation of Tg over exposure. A) Epoxy A. B) epoxy B. C) epoxy C Tg fluctuation over hygrothermal exposure (Choi 2011).

Zhou and Lucas (1999) investigated plasticization and Tg recovery for three different epoxy systems (DGEBA+mPDA, TGDDM+DDS, and Fiberite 934). Samples were fully cured and then immersed in 45, 60, 75, and 90^{o}C water for 1530 hours (63.75 days). Samples were weighed to measure water absorption and appeared to be fully saturated after 45 hours of exposure and maintained a constant amount of water thereafter (depicted in Figure 2-16A). Upon reaching full saturation the Tg was found to have reached its lowest value (measured by TMA); this was followed by a slow recovery of Tg for the rest of the 1530 hours, increasing on average 15^{o}C from the lowest Tg. Recovery of Tg during exposure was more prevalent with increased exposure temperatures, although the amount water absorbed was similar between different temperatures. Figure 2-16B illustrates Tg recovery following full water saturation of 90^{o}C immersed samples.

Once the 1530 hour exposure was complete, specimens were placed in a 60^{o}C oven for 1450 hours to desorb the water. During the desorbing process samples were periodically weighed to detect the amount of water that had been removed from the sample. After 1450 hours in the oven, the original pre-exposure Tg was completely recovered by all epoxy types as presented in Table 2-3. Small amounts of residual water remained and required a higher temperature of 140^{o}C to completely remove. During the desorbing process, the activation energy (heat energy/mol) required to remove water was measured; majority of the water was removed with about 10 kcal/mol, while the residual water required about 15 kcal/mol.

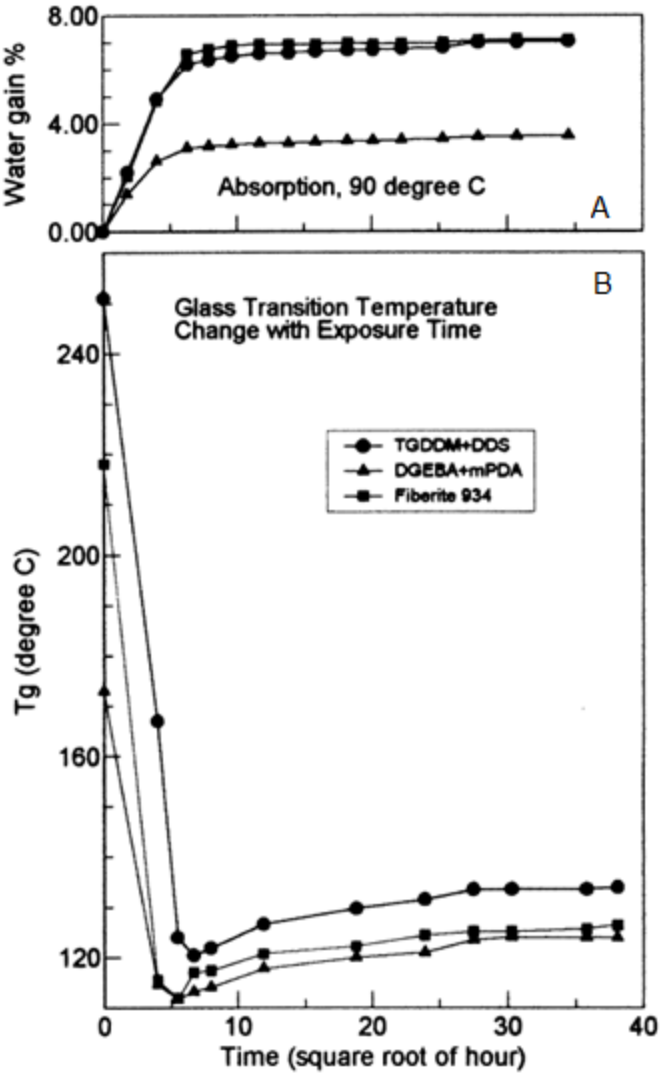

Figure 2-16. Property measurements for three epoxy systems exposed to 90°C water up to 1530 hours. A) Water absorption. B) Tg (Zhou and Lucas 1999).

Table 2-3. Tg of the three epoxies at different stages.

Epoxy	Control (fully cured) (°C)	Immersed at 60°C for 1530 hrs	Desorbed at 60°C for 1450 hrs	Desorbed at 60°C for 1450 hrs and 140°C for 240hrs
TGDDM+DDS	251	108.5	250	251.5
DGEBA+mPDA	173	98	173	173
Fiberite 934	218	106	218	219

Zhou and Lucas (1999) proposed that the two different activation energies were representative of two different types of water interaction within the epoxy. Type I bound

water corresponded to water molecules that bond with epoxy resin hydroxyl groups via one hydrogen bond and was associated with the lower activation energy (Figure 2-17A). Type I bound water was explained as the type that causes plasticization by breaking inter-chain Van der Waals forces, expanding the free volume of the epoxy network, and thereby increasing chain mobility. Type II bound water was hypothesized as the owner of the higher activation energy and was believed to cause secondary cross-linking by forming hydrogen bonds between two polymer chains as illustrated in Figure 2-17B.

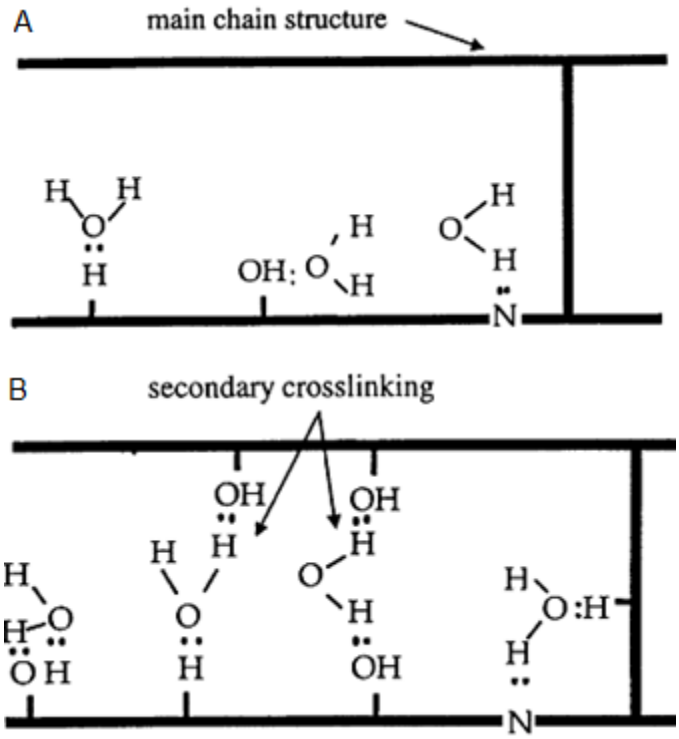

Figure 2-17. Possible bound water complexes. A) Type 1: water molecules form one hydrogen bond and have a lower activation energy. B) Type 2: water molecules form more than one hydrogen bond and have a higher activation energy (Zhou and Lucas 1999).

Type I was partitioned as majority of the absorbed water, and associated with initial saturation of samples, resulting in the large depression of sample Tg. Type II bound water was found to increase with longer immersion time and higher temperatures; cross-linking after the full saturation of specimens. Higher immersion

temperature and longer exposure time resulted in the greater amounts of Type II bound water (considered to be the residual water) remaining after 1450 hours in the 60°C oven. Type II secondary cross-linking was believed to cause the slight Tg recovery over exposure from the initial drop in Tg as imaged in Figure 2-16. Previous research, current design guidelines, and understanding of epoxy behavior and testing provided the foundation of the research approach.

CHAPTER 3
RESEARCH APPROACH

Testing the susceptibility of FRP composites to moisture degradation is often accelerated by increasing the temperature of the environment. Increasing the temperature also increases the rate at which moisture is absorbed and promotes impairment of mechanical properties. Ideally, if a single mode of degradation is activated, then Arrhenius relationship could be used to extrapolate the long-term performance of the composite. This approach is commonly used in GFRP composite reinforcing bars. The Tg for reinforcing bars is typically well above the elevated temperature used for accelerated conditioning.

Cold-cured epoxies used in CFRP composite repair systems, however, typically can have Tg values lower than 60ºC when cured under ambient conditions. Exposure to elevated temperatures above Tg during accelerated aging would not only reduce epoxy stiffness, but could also change the value of the Tg itself. This makes it difficult to determine whether the epoxy ever reached a rubbery state during exposure since the Tg is unknown. This research tracks how the Tg of epoxy samples vary during exposure and investigates the degree added cure and plasticization evoked those changes.

Figure 2-3B demonstrates the importance of knowing the epoxy mechanical properties during exposure and testing. If the epoxy stiffness reduces it will not be able to transfer as much load between the concrete and FRP composite as it did in a glassy state (Figure 2-3A). Reduction of epoxy stiffness and changes in Tg must be considered whenever accelerated aging methods are exercised in FRP composite testing.

The purpose of this research was to understand epoxy Tg fluctuation due to various types of exposure and to investigate the impact of added cure and plasticization

on these fluctuations. Results from this project supplement University of Florida FRP beam testing, providing information on post exposure epoxy characteristics. In combination with the beam project, this research aimed to improve understanding of FRP systems and how they may behave following years of environmental exposure.

Selection of Tg Test Method

The Differential Scanning Calorimeter (DSC) was selected to calculate sample Tg values. Unlike other thermal analysis equipment as detailed in Chapter 3, the DSC does not depend upon mechanical manipulation to detect thermal transitions and is the only method that can calculate Tg via a solely thermal process. This unique capability was important because conditioning of epoxy bond samples as required by AASHTO and ICC codes, and as performed in the beam project, do not incorporate any mechanical loading. That is, such epoxy bond samples are simply placed in conditioning environments for a specified duration under no load. Once conditioning is complete samples are analyzed under various load testing such as tension pull off, or three point bending. However, changes to the epoxy properties such as Tg, cross-link density, and plasticization, occur during conditioning when no load is present. Therefore, the DSC purely thermal calculation of Tg relates well to the epoxy property state over the course of exposure, prior to loading.

Another advantage of calculating Tg with the DSC, is the small sample size. To test samples in the DSC, only 5 to 10 mg epoxy specimens can be used. Such small DSC samples are much more similar in size to epoxy that forms mechanical interlocks on the concrete surface compared to large bar samples as required by other test methods such as the DMA and TMA. Consequently, Tg behavior of small DSC samples

should be very comparable to that of epoxy that forms the bond between the FRP and the concrete.

Selection of Exposure Conditions

Selection of test parameters was motivated primarily from previous research and code requirements as presented in Chapter 3. This research experimented with varied exposure lengths, temperatures, moisture conditions, and epoxy types. Specific test parameters where chosen to extrapolate previous data, analyze the effects of code testing requirements, and to expand knowledge of epoxy behavior under field environments.

Effects from short term exposure (less than 2 weeks) have been well documented in previous research (Choi 2011; Moussa et al. 2011). Exposure durations of 2, 4, 8, and 12 weeks were selected to understand how epoxy samples behave during required code testing as detailed Chapter 3. Collection of 2 and 4 week data allowed comparisons to data from prior research, while 8 and 12 week results developed understanding for epoxy behavior following long term exposure as found in older FRP repairs.

Study of current code standards and previous research illustrates the immense influence of temperature on epoxy behavior and bond strength. Elevated temperatures can not only transition epoxy from a rubbery to a glassy state, but it can also increase the Tg of the epoxy through added curing. Understanding how temperature incites changes in Tg depends on what the temperature is relative to Tg follow ambient cure. To observe how temperature affects Tg, a temperature below and near reported Tg values should be investigated. This research selected 30°C and 60°C temperatures for exposure. A temperature 30°C was chosen because it is above ambient curing

temperature (approximately 23°C) and below characteristic reported Tg values of epoxies tested (listed in Table 3-1). Selection of 60°C was motivated by knowledge that ICC and AASHTO call for this temperature during exposure, its close proximity to the highest temperature ever recorded in the United States (57°C in Death Valley, CA), and because it is near or slightly above manufacturer reported Tg values (listed in Table 3-1).

As suggested by ACI, there is such a deficiency of knowledge concerning epoxy behavior under moist environments. In addition to temperatures above Tg, exposure to moisture can be detrimental to bond strength (ACI Rep. No. 440-07 2007). In field applications FRP composites are exposed to rain, humidity, and even water immersion such as wrapping bridge piles. Although rain is temporary, imagine Portland, Oregon which experiences over 164 rainy days a year or Orlando, Florida which hosts and afternoon yearly average of 89% relative humidity (RH) (Osborn 2013; Florida Climatic Center 2013). In these types of locations plasticization of epoxy is certainly possible. Prior Tg research either did not test humidity conditioning or incorporated it with UV radiation such as Stewart, AASHTO, and ICC standards. This research exposed samples to complete water immersion as well as 100% RH (without UV radiation). With two separate moisture conditions, the effects of plasticization between the two were compared.

Heat and immersion conditioning were combined into one simultaneous exposure, referred to as hygrothermal conditioning. Tg fluctuations caused by added cure were separated from those due to plasticization by analyzing the conversion of the sample (effected by added cure only) in FTIR. After calculating the change of Tg due to

added cure, the remaining change was attributed to plasticization of the sample. Other causes exist, such as different levels of hydrogen bonding, but most researchers consider these effects to be negligible (Stewart 2012; Choi 2011).

Epoxies Tested

The current code specifications provide guidelines intended for all epoxy products in FRP composites (AASHTO LRFD Bridge Design 2012; ACI Rep. No. 440.2R-08 2008; ICC AC125 2012). Six different epoxies provided by five separate commercial manufacturers were tested to study conditioning effects on general epoxy behavior (shared by all six products) and localized behavior (unique characteristics between product types). Relevant properties to this study as reported by manufacturers are summarized in Table 3-1.

Table 3-1. Epoxy properties as reported by manufacturers.

		Property and ASTM Followed		
Epoxy	Cure Conditions	Tg (^{0}C) (ASTM)	Tensile Strength (psi) ASTM D638	Tensile Modulus (psi) ASTM D638
A	3 days, 60^{0}C	82 (D4065)	10,500	461,000
B	5-14 days, 23^{0}C, 50% RH	46 (N.S.)	8,000	250,000
C	Time N.S., 20^{0}C, 40% RH	71 (N.S.)	8,000	440,000
D	56 days, ambient	54 (1356)	10800 (ASTM D3039)	355, 000 (ASTM D3039)
E	7 days, 23^{0}C, 50% RH	N.S.	3,600	650,000
F	N.S.	N.S.	1,770	270,000

N.S. =Information not specified by manufacturer.
RH = Relative Humidity

Epoxy A is a two part epoxy matrix designed for wet-layup fabric FRP composites. Part A and B are mixed at a 100:34.5 weight ratio. A clear and order less resin; it serves as a prime coat, fabric saturant, and/or finish coat depending upon the

application. Following curing at 60°C for 72 hours, it exhibits properties as reported by the manufacturer in Table 3-1.

An impregnating resin and prime coat, epoxy B is two part epoxy also installed with wet-layup fabric FRP composites. By weight, parts A and B are mixed at a 100:34.5 weight ratio. Strength and modulus are taken after a 14 day cure at 23°C and 50% RH, while Tg is calculated following 5 days under 23°C and 50% RH.

Epoxy C is solely applied as an impregnating resin for glass, carbon, or aramid fabric FRP composites. Once saturated in epoxy C, fabric FRP composites are cured into laminates prior to installation. Epoxy C has a low viscosity, low odor and is mixed at a 100:30 weight ratio. After curing at 20°C with 40% RH (length not specified), the manufacturer reports characteristics listed in Table 3-1. Unlike like other resin epoxies tested (A, B, and D) which are clear, epoxy C is opaque.

Epoxy D is a model system, of publicly available consistency. A two part, transparent resin, with no commercial admixtures, epoxy D is composed of diglycidyl ether of bisphenol A (DGEBA, EPON 826) and poly(oxypropylene) diamine (POPDA, Jeffamine D-230). Mixing at a ratio of 100:32.9 by weight respectively, produces a resin of similar appearance and consistency to epoxies A, B, and C. Tensile strength an modulus listed in Table 3-1 were experimentally determined in previous research (Stewart 2012), and the Tg listed was determined in this work.

An opaque paste, Epoxy E is a general structural adhesive, primarily intended for bonding laminate FRP composites or steel plates to concrete, masonry, stone, wood or steel. Parts A and B are mixed at a 100:33.3 weight ratio. The manufacturer did not test for Tg values, but did provide the heat deflection temperature (HDT) via ASTM D648 of

47.8ºC, following 7 days of ambient cure at 50% relative humidity. Water absorption after 7 days of immersion (temperature not specified) of 0.03% (following ASTM D570) was also reported. Epoxy F is another opaque structural paste recommended for sealing and leveling substrate surfaces prior to FRP composite installation. Parts A and B are mixed at a 100:30 weight ratio. Unfortunately no Tg or HDT is provided by the manufacturer.

Test Matrixes

Exposure conditions previously discussed were selected for determining Tg by means of DSC testing. The DSC exposure matrix presented in Table 3-2, summarizes condition selections. Note that each epoxy type had one sample tested for each exposure condition, yielding 6 test specimens per condition.

FTIR specimens were also tested to provide insight to DSC results by providing data for calculation of specimen conversion and water absorption. The exact exposure conditions experience by DSC samples were implemented, but only 2 and 8 week specimens were required to gain understand of specimen behavior. Only 2 week samples were tested for 60° C immersed samples. This decision was based on prior research that reported of plateaus in conversion and water content under this condition after 4 days of exposure (Choi 2011). Paste epoxies were unable to be tested in the FTIR due to the nature of the test (detailed in Chapter 6), leaving resin epoxies A, B, C, and D for FTIR testing. Table 3-3 displays the FTIR exposure matrix.

To enhance understanding of epoxy Tg behavior under required code testing (AASHTO LRFD Bridge Design 2012; ACI Rep. No. 440.2R-08 2008; ICC AC125 2012) and field applications, effects of hygrothermal conditioning were studied. DSC testing permitted specimen Tg to be tracked during exposure. To aid explanation of Tg

fluctuations, FTIR testing was implemented to calculate specimen water absorption and conversion.

Table 3-2. DSC exposure matrix.

Exposure Type	Conditions	Temp. (°C)	Exposure Time (weeks)	Number of Specimens
Control	Atmospheric, 20-28% RH	23-25.5	12	6
Immersion	Water	30	2	6
			4	6
			8	6
			12	6
		60	2	6
			4	6
			8	6
			12	6
Humidity	100%RH	30	2	6
			4	6
			8	6
			12	6
		60	2	6
			4	6
			8	6
			12	6

Table 3-3. FTIR exposure matrix.

Exposure Type	Conditions	Temp. (°C)	Exposure Time (weeks)	# Specimens
Control	Atmospheric, 20-28% RH	23-25.5	12	4
Immersion	Water	30	2	4
			8	4
		60	2	4
Humidity	100%RH	30	2	4
			8	4
		60	2	4
			8	4

CHAPTER 4
DIFFERENTIAL SCANNING CALORIMETER THEORY AND TECHNIQUE

To observe Tg fluctuations over the course of exposure, specimens were tested in a EXSTAR6000 Differential Scanning Calorimeter (DSC) station from Seiko Instruments Inc. equipped with a 220CU module and automatic gas cooling unit. The DSC is a thermodynamic analysis machine that is capable of measuring first and second order thermodynamic transitions with precision.

Review of Thermodynamics

To properly explain how the DSC works, a review of basic thermodynamics is imperative. Thermodynamics studies the transfer of energy between a system with a defined boundary and its surroundings outside of that boundary. The total energy of any thermodynamic system is called enthalpy, which is the sum of all potential and kinetic energies within the system and is normally expressed in joules (J). In thermodynamics, enthalpy, commonly known as *H,* of a system equals the sum of its internal energy and the product of its pressure and volume.

Endothermic and exothermic reactions or processes can change the enthalpy of a system. An endothermic process absorbs energy from surroundings to conduct a chemical or physical change, yielding a $+\triangle H$ of the system, increasing enthalpy. Exothermic processes release heat when performing a chemical or physical change, reducing the enthalpy of the system, $-\triangle H$. These processes are illustrated in Figure 4-1.

An example of an endothermic process is when a crystalline structure melts from a solid to a liquid state. This physical transformation is characterized as a first order thermal transition. A first order transition is defined to include both latent heat and a change in specific heat capacity. As a material is slowly heated, the energy increases

the temperature of the sample. Once near the melting point, heat is still applied, but the temperature of the material stops increasing momentarily as the heat energy is absorbed in the breakdown of the crystalline structure, rather than increasing the sample temperature (Figure 4-2). This heat absorption is considered latent heat.

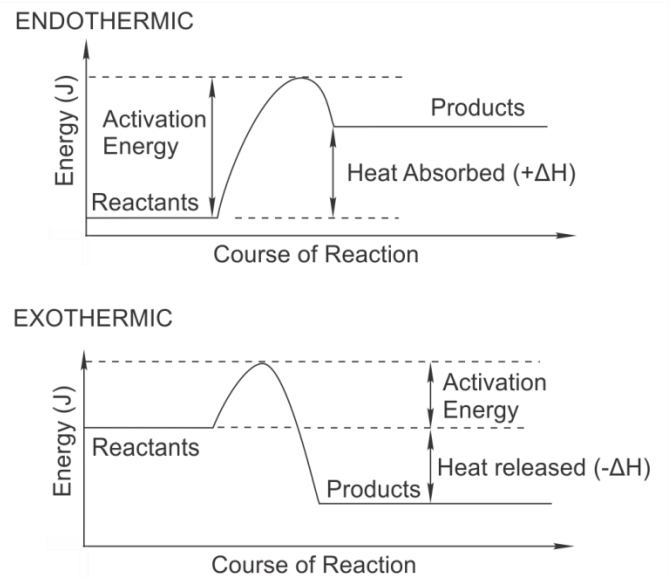

Figure 4-1. Endothermic and exothermic energy processes.

Unlike crystalline structures, amorphous polymers such as epoxy have a Tg rather than a melting point, which involves neither a endothermic nor endothermic process. The physical transition from a glassy state to a rubbery state is considered a second order thermal transition, identified solely by a change in specific heat capacity (Figure 4-2). Specific heat capacity, c_p, is the heat or energy required to raise a unit of mass by one unit of temperature and is commonly expressed as joules per kelvin per kilogram (J/K/kg). Therefore, more energy is required to raise a polymer in a rubbery state by one degree of temperature than was required in a glassy state.

Note in Figure 4-2, that Lh represents the latent heat absorbed in a crystalline material and that cp1 and cp2 are the specific heat capacities before and after the

transitions respectively. As Figure 4-2 illustrates, both first and second orders experience an increase in specific heat capacity following transition, but only first order transition hosts any latent heat. This latent heat is the energy absorbed into the system, explaining the endothermic behavior of melting. The DSC utilizes the change in heat capacity during the glass transition as presented in Figure 4-2 to measure the Tg of epoxy samples.

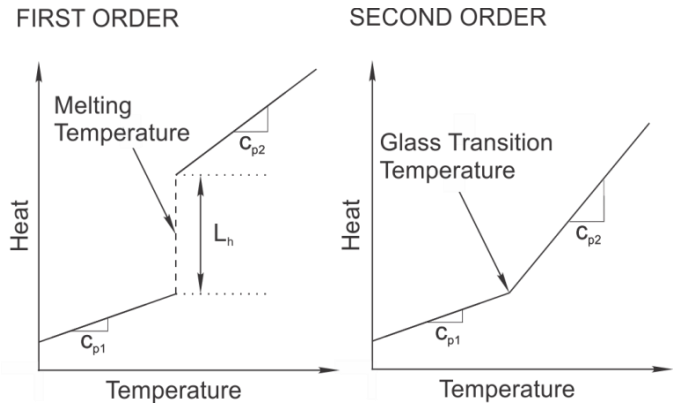

Figure 4-2. First and second order thermal transitions.

DSC Theory

The DSC detects changes in heat capacity and endothermic/exothermic processes by measuring heat flux, which is the rate of heat transfer through a given surface. The DSC test chamber holds a specimen inside a sample container and an empty container as a thermal reference. Components of the test chamber are detailed in Figure 4-3. The operator inputs a temperature cycle for the temperature program. The temperature program controls the temperature of the heat sink using heaters and liquid nitrogen. The heat sink is designed to maintain uniform temperature over the heat conducting surface of the chamber. Temperature is conducted from this surface through the thermal resistant posts into the sample and the reference, increasing or decreasing their temperature. Heat flow (joule/sec or Watts) transferring through the thermal

resistant posts is measured and is proportional to the temperature difference between the heat conducting surface at the bottom and the container at the top.

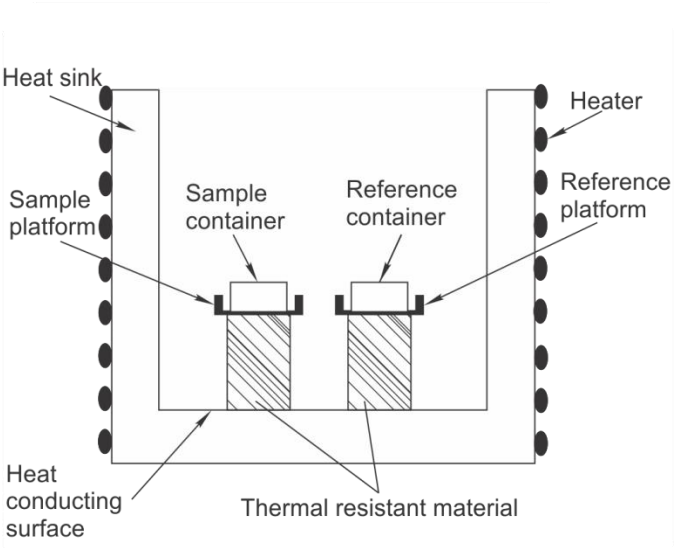

Figure 4-3. DSC test chamber.

The DSC varies the sample and reference temperature at identical rates according to the specified temperature program, normally 10°C per minute as recommended by ASTM 1356-08. Because the sample container has more mass than the empty reference container, more heat flow is required to keep the sample at the same temperature as the reference. The difference between the heat flow (μW) to the reference and the sample is measured and stored as the temperature changes. This heat flow difference is typically plotted as a function of the temperature to form the DSC curve. If the sample undergoes thermal transitions (illustrated in Figure 4-2), the DSC curve can be used to determine melting temperatures or Tg.

DSC example curves are depicted in Figure 4-4. The slope and magnitude of the heat flow difference is related to the thermal contact between the thermal posts and sample or reference and are not used quantitatively to determine Tg or melting point. Note that both curves have negative heat flow difference, which indicates that the

sample requires more heat energy than the reference to increase temperature at the same rate.

Areas formed by the DSC curve represent either an exothermic or endothermic processes. For example the negative area formed by the DSC curve in Figure 4-4A represents an endothermic reaction, in this case melting. Initially the heat flow difference is linear but then latent heat (represented by the area formed by the DSC curve) is absorbed during transition from solid to liquid, therefore additional heat flow is required to maintain the temperature increase rate illustrated by the drop in the DSC curve. Once melting is complete the heat flow difference becomes constant again. An exothermic process causes the heat flow difference to increase temporarily and forms an area above the baseline.

Glass transition is characterized by a step change in the DSC curve baseline (Figure 4-4B). Before the glass transition occurs, the DSC curve displays a constant heat flow difference of -0.2 mW. Immediately after glass transition, the heat flow difference is a constant -0.35 mW. The increase in heat flow difference is proportional to the increase of specific heat capacity that occurs once an amorphous polymer transitions from glassy to rubbery.

Often during epoxy DSC testing, an endothermic area also appears in conjunction with the glass transition step change, as portrayed Figure 4-5. This area is the result of enthalpy relaxation as the temperature of the epoxy increases. Initially, when the epoxy structure cured, internal pulling and pushing forces were created. These forces are internally trapped in the epoxy matrix as potential energy. As the glass transition temperature is approached and epoxy is about to transition into a rubbery

state, heat is absorbed into the epoxy matrix to release these internal forces resulting in an endothermic curve.

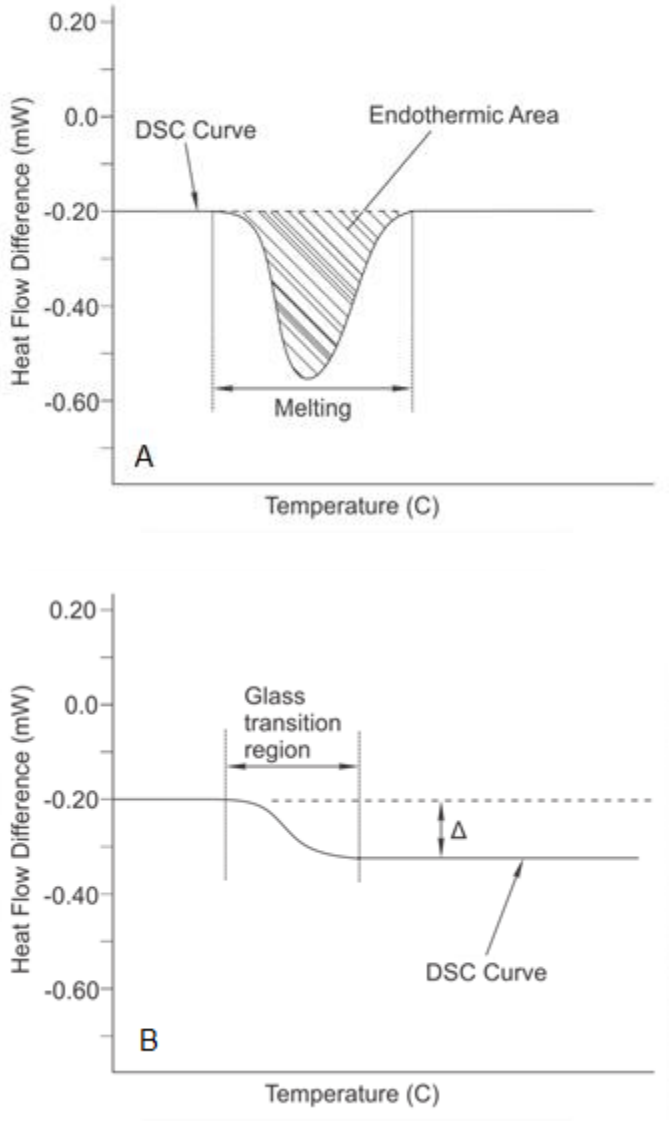

Figure 4-4. DSC examples curves. A) DSC curve during melting. B) DSC curve during glass transition.

The degree of enthalpy relaxation is determined by the thermal history of the epoxy specimen. If the specimen is exposed to temperatures near or above the Tg then enthalpy relaxation is relieved during conditioning by transitioning into a rubbery state, prior to DSC heat cycles. Consequently, the DSC curve will have no enthalpy relaxation

area. Figure 4-6 displays two DSC curves from this research to compare enthalpy relaxation of samples with different thermal histories. Both were exposed to 100% RH for 2 weeks. Notice that the enthalpy relaxation area of the specimen exposed to 60°C is much smaller than that of the 30°C specimen. This curve behavior suggests that for this epoxy, the 60°C exposure was close to or over the Tg.

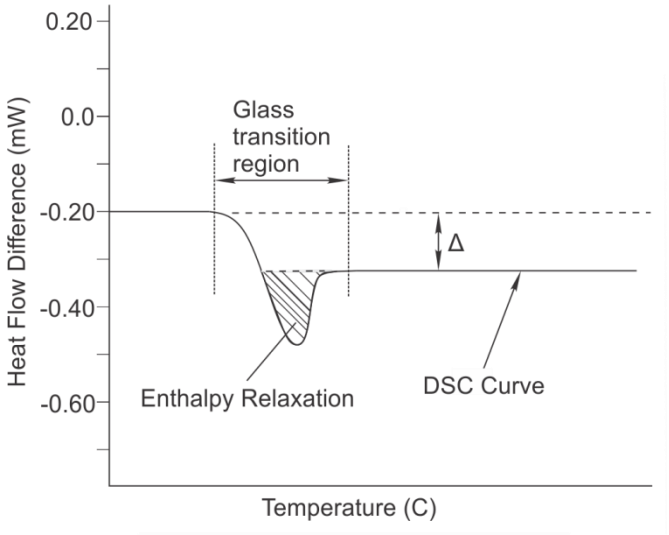

Figure 4-5. DSC example curve of enthalpy relaxation.

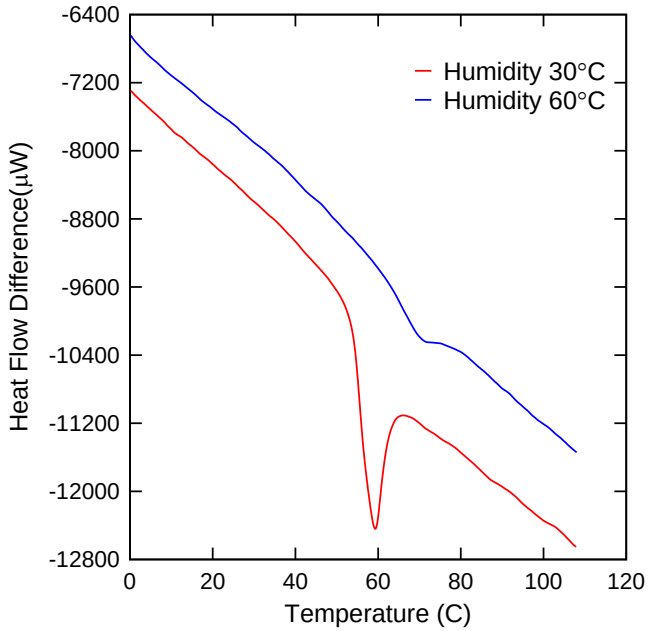

Figure 4-6. Enthalpy relaxation with different thermal histories.

Tg Calculation

ASTM 1356-08 provides guidelines to analyze a DSC thermal curve to define a specific glass transition temperature. ASTM 1356-08 provides Figure 4-7 as an example thermal curve to demonstrate Tg calculation. Note that the upper curve is the difference in heat flow between the sample and the reference and lower curve is the derivative of the heat flow difference.

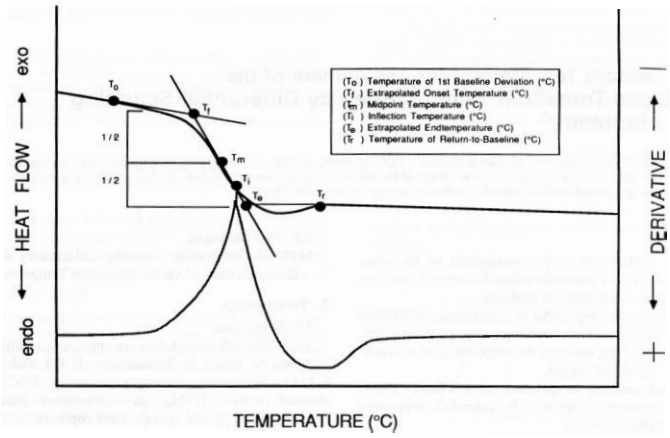

Figure 4-7. ASTM 1356-08 example thermal curve.

As the upper curve in Figure 4-7 illustrates, there is a linear base line in the thermal curve on either side of the step change where the heat flow maintains a constant slope. On left side of the step change, the sample is in a glassy state where the covalent bonds of the epoxy are locked and “frozen” in place. During the step change, covalent bonds begin to loosen and gain liberty to rotate. In this region, the epoxy specific heat capacity increases, creating the drop in the DSC curve. This step is the glass transition region. To the right of the step change in the thermal curve, the epoxy is in a consistent rubbery state. In this rubbery state, the epoxy will have less structural stiffness as it did in the glassy state. The glass transition temperature is defined as the temperature at which this change in epoxy stiffness begins.

ASTM 1356 provides a graphical method to calculate Tg. Initially 3 lines are constructed over the thermal curve: two lines to extrapolate each base line into the step change region and then a third line drawn tangent to the point of greatest slope on the glass transition curve as illustrated in Figure 4-7. The intersection of the extrapolated baseline prior to transition and the slope tangent line is labeled as Tf, and is defined as the extrapolated onset temperature. Likewise, Te is the intersection of the extrapolated baseline following the transition curve and the tangent and is defined as the extrapolated end temperature. The midpoint temperature, Tm, is taken as the point on the curve associated with half of the heat flow difference between Tf and Te.

ASTM 1356 notes that the glass transition of materials occurs over a range of temperatures and that Tf, Tm, or Te can be chosen to represent the specific glass transition temperature. It mentions that Tm is the preferred value to be selected as the glass transition temperature and is the most comparable value to other techniques employed to find Tg. This research will take the Tg of every sample to be equal to Tm, the midpoint temperature of the glass transition region.

It is important to note that ASTM 1356 is a guideline for generic Tg calculation and is not specific to epoxies. It mentions that if appropriate, an initial heat cycle can be performed up to 20ºC above the expected Te to remove any unwanted thermal history from the sample, followed by a second heat cycle to determine Tg. This guidance is not appropriate for calculating the Tg of epoxy specimens. If an initial heat cycle was performed, the specimen would experience additional cure and exhibit a larger Tg during the second cycle than the specimen really had prior to testing. Consequently it is

pertinent that the Tg is calculated from the first heat cycle experienced by the sample to maintain accurate results.

Sample Preparation

Alodined (chromate corrosion inhibiting) pans and covers were selected to hold epoxy specimens during DSC testing. These small containers were less than a quarter of an inch in diameter and held no more than 10 mg of epoxy. One individual pan and cover is shown in Figure 4-8. The parts A and B for each system were mixed according to the manufacturer's specified mixing ratio in a smooth plastic container shown in Figure 4-9. All photos provided by Paige Blackburn for the remainder of this chapter.

Figure 4-8. Alodined pan (left) and cover (right). Photo provided by Paige Blackburn.

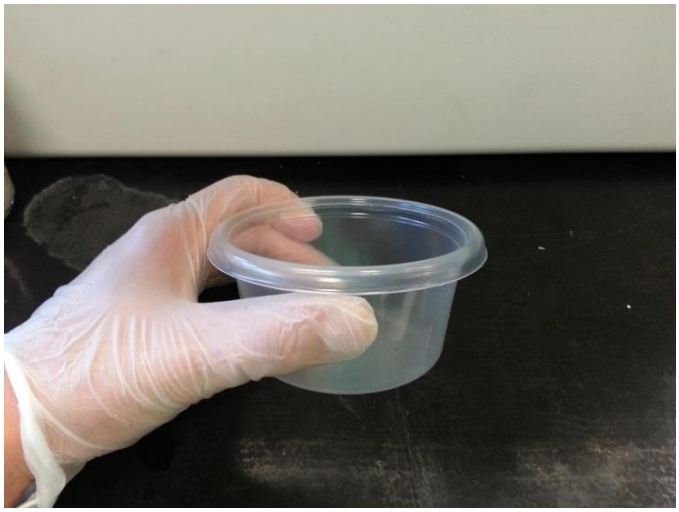

Figure 4-9. Container used to mix epoxies. Photo provided by Paige Blackburn.

Once the correct ratios of parts A and B were combined, the epoxy was mixed rapidly for four minutes, ensuring that the epoxy was completely uniform in appearance. Figure 4-10 displays epoxy E after mixing was complete.

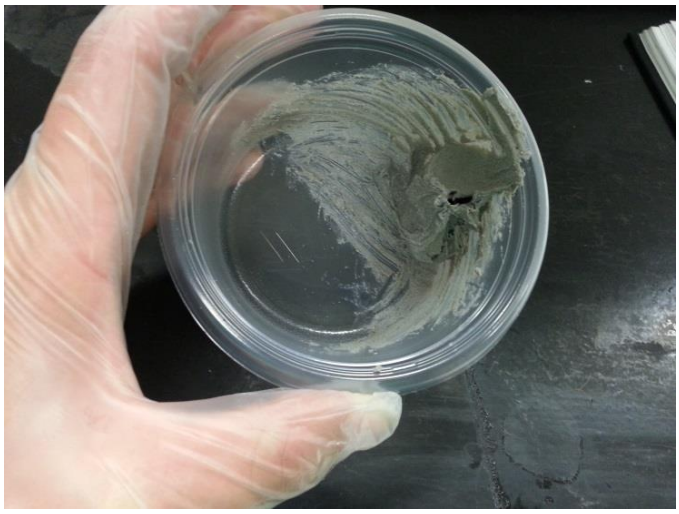

Figure 4-10. Epoxy E after mixing. Photo provided by Paige Blackburn.

Immediately after mixing was complete a single epoxy sample was created for a zero cure test. Once the zero cure sample began testing in the DSC, the remaining epoxy samples were constructed. For the resin epoxies, samples were created by carefully placing 3.75 mg to 6.25 mg of mixed epoxy into the bottom of an alodined pan, shown previously on the right in Figure 4-8, with a steel needle and syringe. For the paste epoxy systems, a tooth pick was selected to carefully place epoxy into pans due to the high viscosity of the pastes. With a tooth pick, 6 mg to 8 mg of paste epoxy was placed into each pan. Epoxy samples were spread and flattened into the bottom of pans with a tooth pick to increase the thermal contact between the epoxy and the pan, maximizing the consistency of DSC results. A completed paste epoxy specimen is pictured in Figure 4-11. Epoxy specimens were allowed to cure for 2 weeks under

ambient conditions and were then transferred to specified exposure conditions (method detailed below).

Figure 4-11. Epoxy E sample. Photo provided by Paige Blackburn.

Pan Crimping

Immediately following exposure (if specified), samples were patted dry (if exposed in water) and prepared for pan crimping. The pan cover, pictured on the right in Figure 4-8, was placed inside a pan containing the epoxy sample as shown in Figure 4-12.

Figure 4-12. Cover and pan prepped for crimping, approximately a 0.25 inch diameter. Photo provided by Paige Blackburn.

Once the cover was perfectly centered inside the pan, it was placed in the appropriate lower dye of an S II Seiko Instruments pan crimper, pictured in Figure 4-13 and Figure 4-14.

Figure 4-13. Pan crimper. Photo provided by Paige Blackburn.

Figure 4-14. Epoxy sample ready for crimping. Photo provided by Paige Blackburn.

To crimp the sample, the upper dye was lowered, crimping the outer edges of both the pan and the cover inward until flat. A crimped sample, ready for testing, is presented in Figure 4-15. Once the cover and the pan were crimped together, the sample was considered to be completely sealed from any leaking, trapping the epoxy inside.

Figure 4-15. Crimped epoxy sample. Photo provided by Paige Blackburn.

DSC Testing

Following exposure and crimping, samples were placed into the DSC to measure Tg. DSC analysis was conducted using an empty pan as a thermal reference as shown in Figure 4-16 as recommended in ASTM 1356-08. The environment inside the DSC chamber was temperature controlled with liquid nitrogen and received a constant flow of nitrogen gas to eliminate any moisture present in ambient air. The temperature cycles were programed to change from the initial chamber temperature (normally 20° C), to -20°C, held for 3 minutes and then from -20° to 120° C, both at a rate of 10° C per minute. The purpose of the temperature range was to allow a DSC base line to form on

either side of the Tg. These baselines were then extrapolated in order to calculate the Tg.

Figure 4-16. Plan view of sample and reference pans inside the DSC test chamber. Photo provided by Paige Blackburn.

Tg Calculation in the DSC

Tg was determined using the Seiko DSC analysis computer software, which followed ASTM 1356. After running a sample through the temperature program, a DSC thermal curve as pictured in Figure 4-17 was produced.

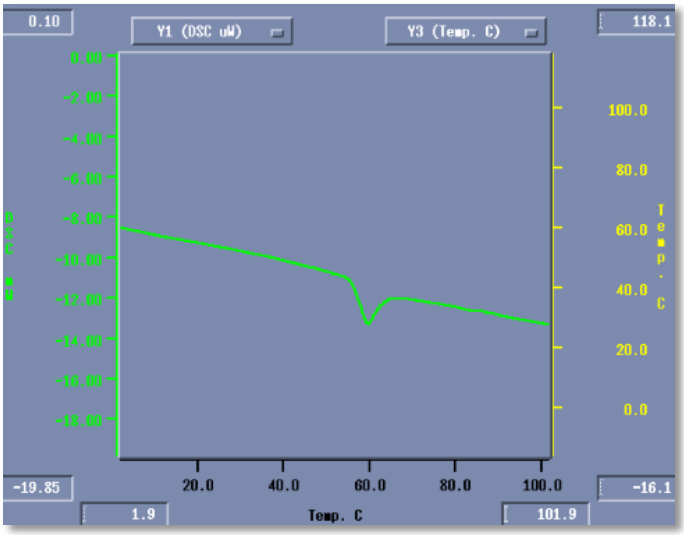

Figure 4-17. Thermal curve in DSC analysis software.

To calculate the Tg, <Glass Transition> was selected from the calculation options in the software. The software prompts the user to select a point along each baseline; it then takes the slope at that point and extrapolates a line towards the step change in the thermal curve. The red cursor lines of Figure 4-18A locate the selection of the point on the first baseline, which the software titles “T1”. Similarly, the right image presents the selection of point “T2”, which the software intakes to calculate the second baseline extrapolation.

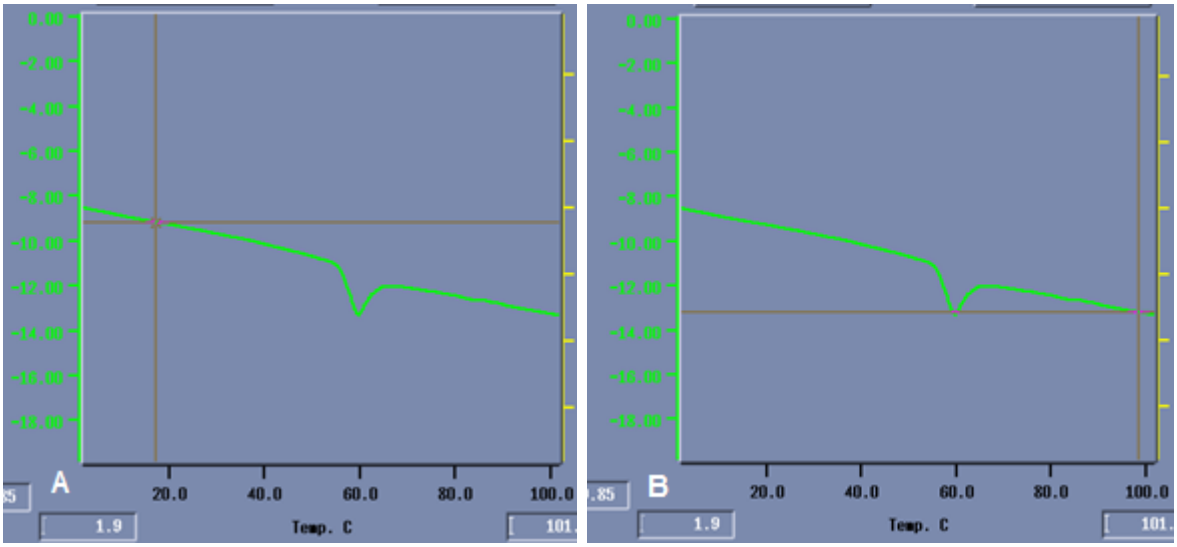

Figure 4-18. Software points selected for baseline extrapolation. A) T1, point prior to transition. B) T2, point following transition.

Following the selection of T1 and T2, the software calculates the greatest slope and its location along the glass transition region and creates a tangent line. Lines are then extrapolated from T1 and T2 until they intersect the tangent line. The software takes the difference in heat flow between these two intersections, divides the difference by two to create an additional point on the tangent line. This point is Tm as defined by ASTM 1356, and is recorded as Tg. Figure 4-19 illustrates the result of this process. In this example the Tg would be taken as 55.9ºC.

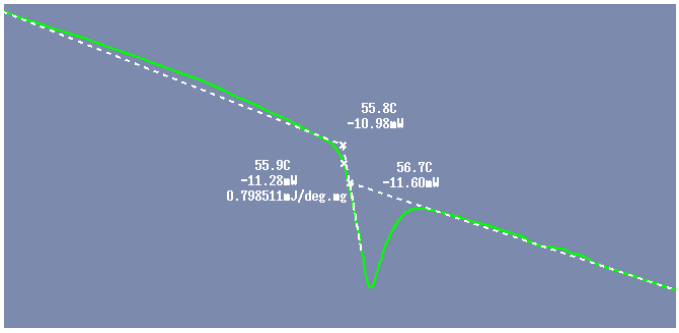

Figure 4-19. Initial software calculation of Tg.

As observed in Figure 4-19, extrapolation from T1 and T2 (white dotted lines) may not perfectly match visually to the actual baselines (green). This difference is caused when the slope at T1 or T2 is not the perfect average slope that best represents the entire baseline. To adjust extrapolations, the point of intersection with the tangent can be moved to create a more accurate extrapolated line. When a point of intersection is selected, both the associated extrapolated baseline and the tangent line will move with point as it is adjusted. Figure 4-20 illustrates the point selection required to adjust the extrapolated baseline. Note that the lines highlighted in black will move with the point.

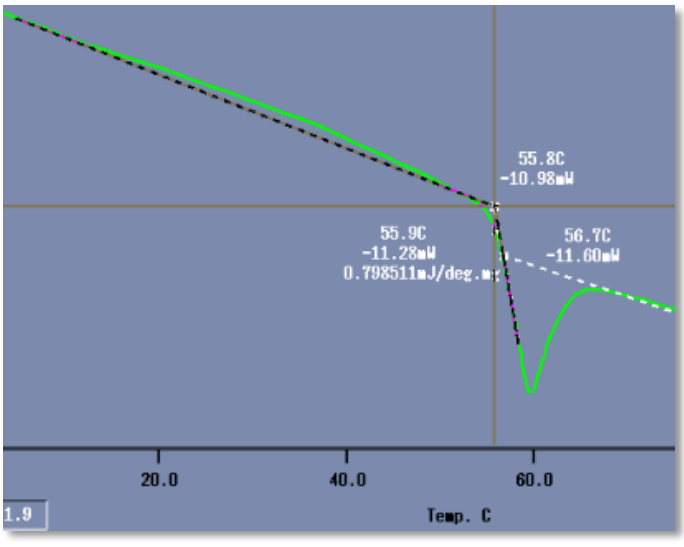

Figure 4-20. Adjustment of baselines in the DSC software.

While maintaining the original slope of the tangent line, the point of intersection was adjusted until the extrapolated baseline best matched (visually) the slope of the actual base line. This process was conducted separately for each baseline. The software recalculates the Tg based on adjustments made. Figure 4-21 displays this recalculation, note that the extrapolated baselines better match the actual baselines when compared to Figure 4-19. With this baseline adjustment, the Tg calculated changed from 55.9ºC to 55.1ºC.

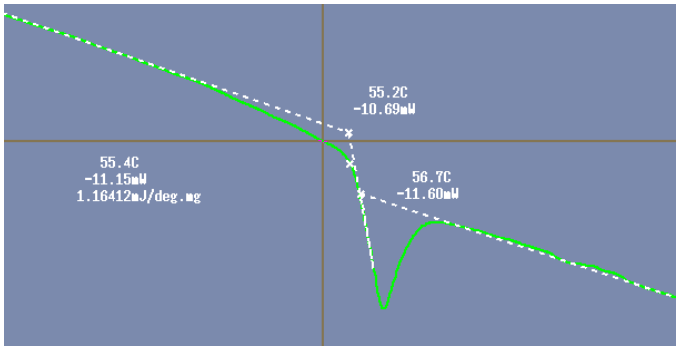

Figure 4-21. Final software calculation of Tg.

Because this adjustment process is visually conducted by the software user, there is human error involved with the nature of this Tg calculation. To ensure the most accurate results as possible, the Tg was calculated repeatedly for each sample, until additional calculations exhibited a less than 2% error than the previous calculation. Once this small error requirement was satisfied, the associated final Tg calculation was recorded as the representative Tg for the sample tested.

CHAPTER 5
EXPOSURE CONDITIONS

Maintaining sample organization during exposure was vital, particularly during when samples could potentially shift and move from their original positions. Samples assigned to the same exposure condition were formed into batches and then prepped and exposed together to maintain organization.

Required Sample Organization

When each sample was tested in the DSC, the correct sample weight was input into the computer software in order to provide the most accurate results. For exposure conditions that included moisture it was possible that the sample weight increased due to the added weight of moisture on the surface of the sample. Although samples were patted dry before testing, the weight entered into the DSC was to the nearest .01 mg; because this is such a small measurement, remaining moisture after being patted “dry” could change the original weight of the sample. Therefore, to get the correct weight of the epoxy itself, without including moisture, the weight of epoxy was recorded during sample creation. The weight of each epoxy sample ranged from 3.75 mg to 8 mg. Because each sample had a different weight that needed to be entered into the computer during testing, they were carefully organized during curing, exposure, and testing.

After samples were created and their weights were recorded, all were allowed to cure under ambient conditions in the dark for a minimum of two weeks. Samples were placed into individual labeled compartments of a plastic box to maintain organization during curing (Figure 5-1). All photos were provided by Paige Blackburn for this chapter.

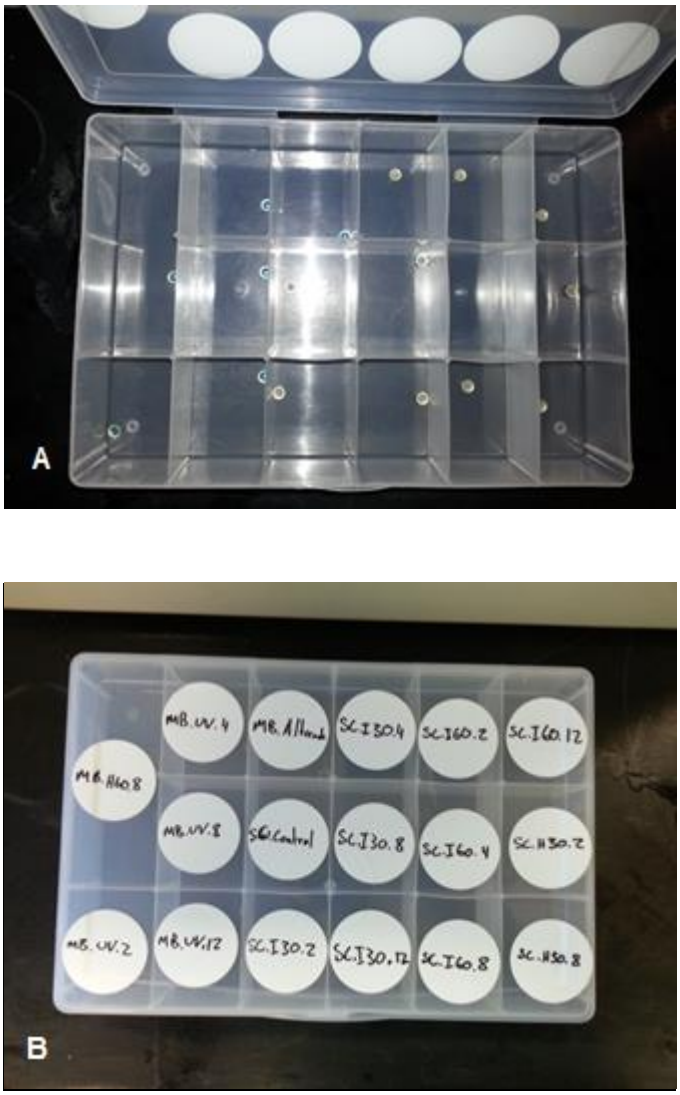

Figure 5-1. Sample Organization. A) Sectioned storage box with epoxy samples. B) Labeled compartments for each sample. Photos provided by Paige Blackburn.

Immersion

Samples specified for water immersion were placed into small 1in x 1in plastic bags, each labeled with a waterproof marker. Each bag was filled with water, given its assigned sample and had any remaining air squeezed out during the sealing of the bag. Prepped bags are shown in Figure 5-2.

Figure 5-2. Labeled bags containing samples. Photo provided by Paige Blackburn.

After the samples were placed in the labeled bags, a compartmentalized plastic box was completely filled with warm water (either 30° or 60° C). Each labeled bag was then placed into an individual compartment of the box (Figure 5-3). The lid of the box was latched and tightly zip-tied shut (Figure 5-4). The box containing the samples was then placed inside of a exposure tank that maintained water at a constant temperature during specified exposure times.

Figure 5-3. Labeled bags in individual compartments of exposure box. Photo provided by Paige Blackburn.

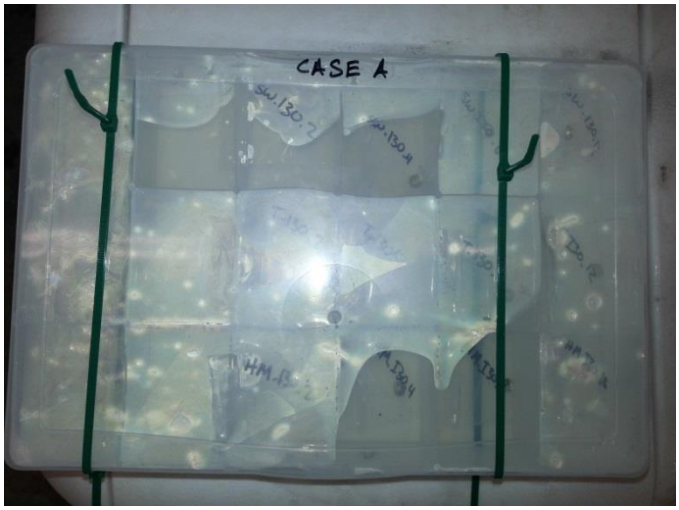

Figure 5-4. Exposure box sealed and ready to be exposed. Photo provided by Paige Blackburn.

Once exposure was completed, the labeled bags were taken out of the exposure box and transported for testing in the DSC. Right before individual testing, the test sample was removed from its respective bag and then patted dry before it was placed into the DSC chamber.

Relative Humidity

Samples specified for exposure to 100% relative humidity at either 30° or 60° C were placed directly into a compartmentalized exposure box. Prior to sample placement, each compartment of the box had two 1/8 inch holes drilled into the bottom in order to allow any water accumulation during exposure to drain out of the compartment. The lid of the exposure box was then held open to maximize sample exposure. This box was placed into the same exposure tank used for immersion, but onto masonry blocks that held the samples out of the water (Figure 5-5). With the lid of the exposure tank closed, the air inside the tank above the water maintained 100% relative humidity. Once humidity exposure was completed, the samples were placed inside a labeled plastic bag and transported for DSC testing.

Figure 5-5. Humidity exposure techniques. A) Samples prepped for humidity exposure. B) Exposure box held out of water inside exposure tank. Photos provided by Paige Blackburn.

CHAPTER 6
FTIR THEORY AND TECHNIQUE

Fourier transform infrared spectrometry (FTIR) was utilized to measure conversion and amount of absorbed water. With a FTIR Nicolet Magna 760 from Thermo Electron Cooperation near-infrared spectra over the range of 3800-6800 cm^{-1} were recorded. Data was formed with 32 scans at a 4 cm^{-1} resolution implementing a white light source, a CaF beamsplitter, and an MCT light detector.

FTIR Theory

The FTIR measures light absorbance into a thin epoxy film sample. Light of varying frequency is emitted through the film sample while light intensity entering and exiting the sample is measured to calculate absorbance. The light frequencies emitted are in the vibrational range of the electromagnetic spectrum as Figure 6-1 presents. In this range light frequencies can incite vibration in molecular functional groups that compose the epoxy film sample.

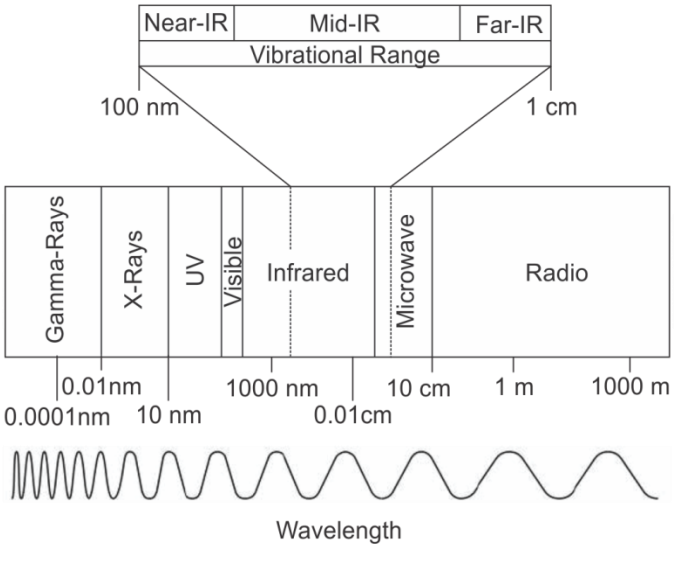

Figure 6-1. Electromagnetic spectrum with vibrational range indicated.

Each type of molecule has a unique natural frequency dependent on the mass of its atoms and the stiffness of its bonds between atoms. A molecule can be modeled as a spring system as Figure 6-2 illustrates, where atoms are masses and bonds are springs. Implementing this approach, the natural frequency of molecules, w, can be calculated with Equation 6-1, where k is the bond stiffness and μ is mass. In a dipole structure as exemplified in Figure 6-2, μ is calculated according to Equation 6-2.

$$w = \frac{1}{2\pi} * \sqrt{\frac{k}{\mu}} \qquad \text{Equation 6-1}$$

$$\mu = \frac{m1*m2}{m1+m2} \qquad \text{Equation 6-2}$$

If the light frequency emitted into the film sample matches the natural frequency of one of the contained molecular functional groups, it results in a vibrational resonance of that particular functional group. If resonance occurs, light energy transitions into vibrational energy, consequently increasing the absorption of light into the sample.

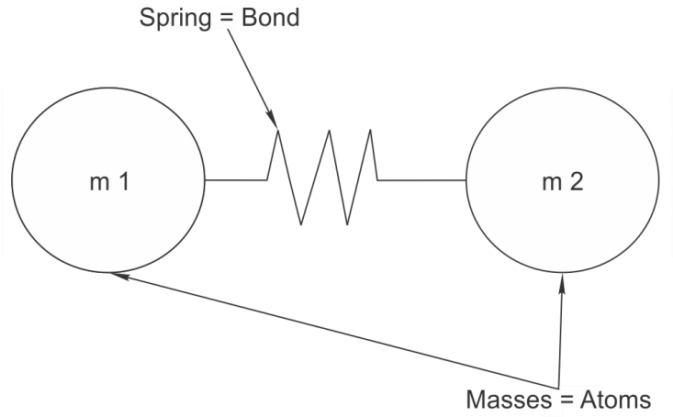

Figure 6-2. Molecular spring system.

FTIR outputs data in the form of spectra presenting light absorbance over the near-IR frequency range (Figure 6-3). As the plot illustrates, peaks in light absorbance coincide with particular wavenumbers on the x axis. Each peak is associated the vibration of a particular molecular functional group, the wavenumber at the peak is the

natural frequency of that specific functional group. Natural frequencies of interest in this research include characteristic water peak at 5230 cm^{-1}, phenyl peak at 4622 cm^{-1}, the epoxide functional group peak at 4530 cm^{-1}, and an unknown peak at 4569 cm^{-1}. These peaks are identified in Figure 6-4.

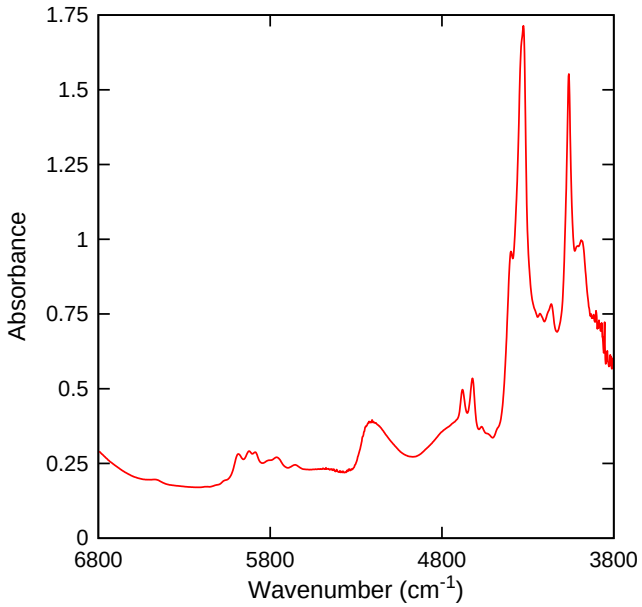

Figure 6-3. FTIR example scan.

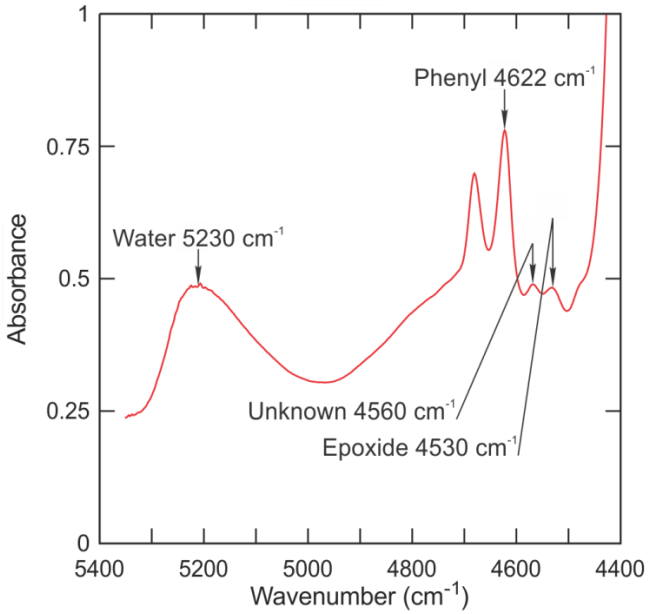

Figure 6-4. FTIR peaks of interest identified.

Area underneath a peak in the FTIR spectra is directly proportional to the amount of the respective molecular functional group present in the film sample. Area underneath the peaks can be used to determine relative quantity of water present and sample conversion. The peaks of interest are detailed below in the data analysis section.

Sample Preparation

FTIR epoxy samples had to be formed into thin films to allow light to pass through. To create films two 8 in x 12 in glass panes were covered in Teflon sheets on one side as presented in Figure 6-5, which were smooth enough to prevent mechanical bonding of the epoxy to the Teflon. This allowed films to be removed easily following curing. Film samples were cured for 2 weeks before exposure. A third piece of Teflon served as a stencil and a spacer to control the film shape and thickness. Two 2in x 2in squares were cut into this Teflon sheet as Figure 6-6 displays. This stencil layer was secured to one of the covered glass panes; providing a platform, illustrated in Figure 6-7, prepared to receive uncured epoxy. All photos were provided by Paige Blackburn for this chapter.

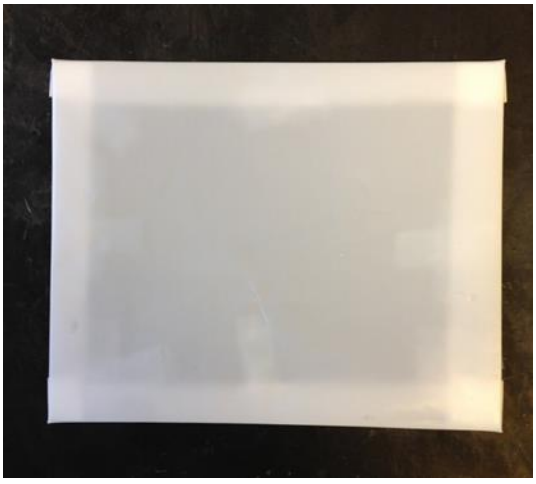

Figure 6-5. Glass covered in Teflon. Photo provided by Paige Blackburn.

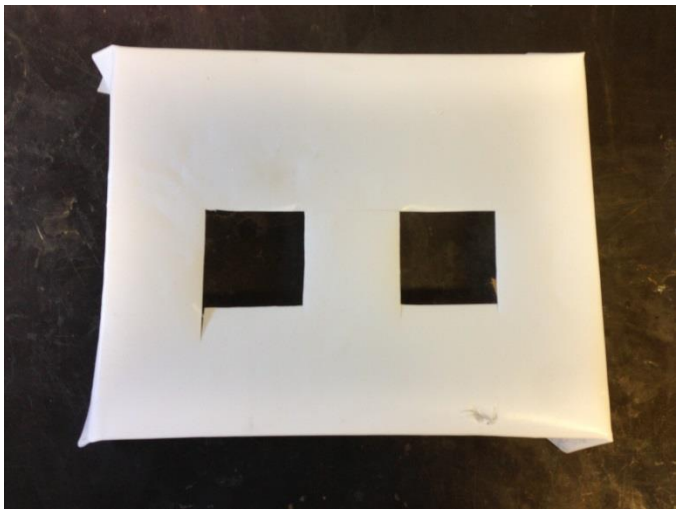

Figure 6-6. Teflon stencil and spacer. Photo provided by Paige Blackburn.

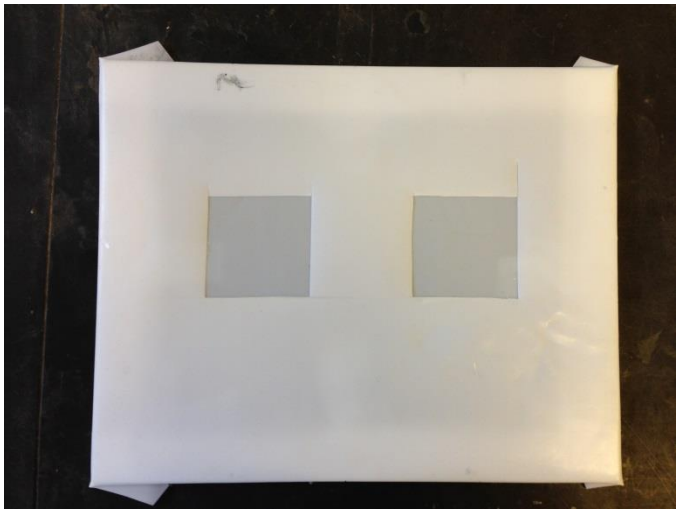

Figure 6-7. Teflon platform. Photo provided by Paige Blackburn.

The parts A and B for each epoxy system were mixed according to the manufacturer's specified mixing ratio in a smooth plastic container (composed of poly propylene) shown in Figure 4-9. Once the correct ratios of parts A and B were combined, the epoxy was mixed rapidly for four minutes, ensuring that the epoxy was completely uniform in appearance. Following mixing, 12 drops of epoxy were placed to Teflon platforms by a syringe. Platforms allowed for two separate film samples to be prepared simultaneously, demonstrated in Figure 6-8. The second piece of Teflon

covered glass was then centered over and placed on the platform. Approximately twenty pounds was evenly distributed over the two pieces of glass to ensure uniform film thickness.

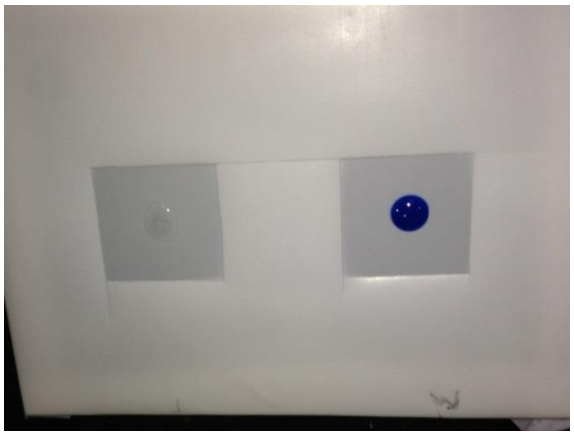

Figure 6-8. Two epoxy samples prepared to be spread into films. Photo provided by Paige Blackburn.

This process yielded film samples that ranged from 0.23 to 0.69 mm thick. Following 2 weeks cure, 2 in x 2 in film samples were cut into approximately 0.5 in x 0.5 in pieces and prepared for exposure (Figure 6-9). Film samples were then exposed according to Table 3-3.

Figure 6-9. Film samples prepared for exposure. Photo provided by Paige Blackburn.

Exposure

FTIR film samples were exposed in a similar manner as DSC samples, detailed in Chapter 5. Immersion film samples were placed inside labeled plastic bags (Figure 6-9) filled with water, and placed inside a compartmentalized box filled with water similar to that presented in Figure 5-3 and Figure 5-4. Compartmentalized boxes were then sealed shut and submerged in temperature controlled tank water. The 100% relative humidity samples were kept in labeled plastic bags which were held open with small slices of wood. Holes were created in the bottom of bags to prevent water accumulation. Bags were held in an opened small plastic container, pictured in Figure 6-10. This container was then held above the water inside sealed temperature controlled tanks, which allowed the air above to reach 100% relative humidity.

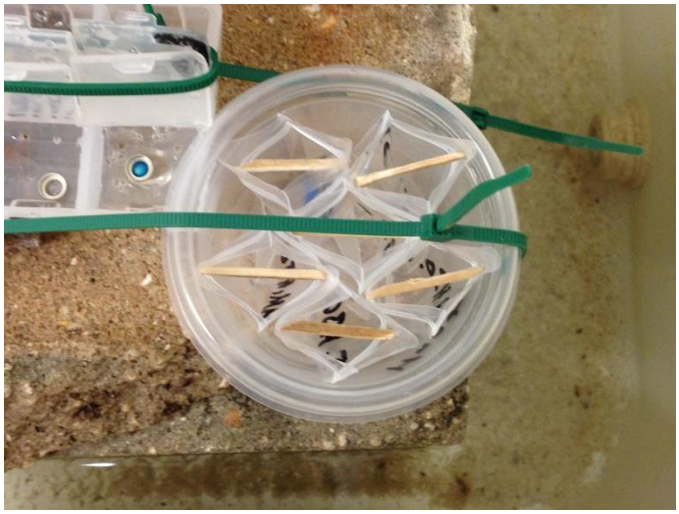

Figure 6-10. Film samples prepared for humidity exposure. Photo provided by Paige Blackburn.

FTIR Test Procedure

Following exposure, samples were transported to the FTIR lab, patted dry, and air dried for at least 5 minutes. Drying was necessary to prevent inaccurate water area to be recorded at the water peak (5230 cm^{-1}).

Near-IR white light source was selected to capture the peaks of interest. Near-IR required a CaF2 beam splitter, which can transfer light frequencies from 14500-1200 cm^{-1}, capturing the entire near-IR range. A MCT/A detector was implemented to measure light intensity due to its broad spectral range that includes most of the near-IR frequencies. The data collection options were set to 32 scans, 4 cm^{-1} resolution, 6800-3800 cm^{-1} spectra range (which contains the peaks of interest) and sample absorbance output displayed on the vertical axis.

Once samples were dried and FTIR settings were programed a background scan was collected. The background scan recorded light absorbance into the environment existing in the FTIR chamber such as air and moisture molecules. Absorbance recorded from the background scan was automatically eliminated from the sample scan performed next. Figure 6-11 presents a typical background scan. Following a background scan an epoxy film sample was placed into the FTIR chamber and a sample scan was collected. Once the sample scan was complete, data were available for analysis.

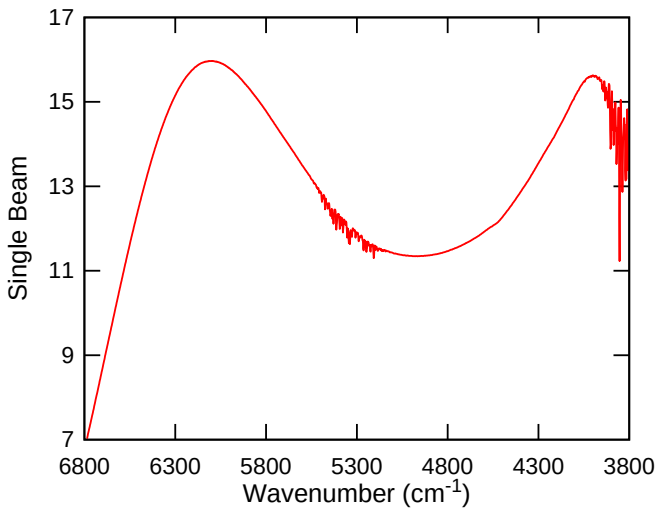

Figure 6-11. Typical FTIR background scan.

Data Analysis

Conversion

The epoxide functional group identified at 4530 cm^{-1} (Figure 6-4), is the monomer composing part A polymer chains, which provides body to epoxy. Part B is the liquid hardener that catalyzes cross-linking between epoxide polymer chains. Covalent bonding alters the molecular form of the epoxide functional group and consequently its natural frequency. Hence, when analyzing FTIR data, the smaller the area of the epoxide peak at 4530 cm^{-1} the larger the conversion of the sample caused by the reduction of epoxide groups during curing. An epoxy sample is considered completely cured (conversion equals 1.0) when no peak exists at 4530 cm^{-1}, indicating that all epoxide groups have reacted with the hardener and no additional covalent bonding opportunities remain within the epoxy structure. Comparison of area underneath the epoxide peak at 4530 cm^{-1} between samples allows conversion to be measured.

To calculate the percent cure of each sample Equation 6-3 was employed. Where α represents the conversion, A(0) is the epoxide area of a zero cure (conversion equals 0.0) sample and A(t) is the epoxide area of a partially cured sample. By subtracting the ratio from 1, the equation provides the fraction of epoxide group that has been converted into the epoxy cross-linked structure.

$$\alpha = (1 - \frac{A(t)}{A(0)}) \qquad \text{Equation 6-3}$$

Areas from FTIR curves required to exercise Equation 6-3 were calculated in OMNIC software. The epoxide peak area overlapped an unknown peak area, as Figure 6-12 demonstrates, which had to be considered to maintain accurate calculations. The unknown peak is an example of band overlapping which can produce inaccurate data

analysis if not properly subtracted (Chike 1993). The unknown peak was subtracted as performed by previous research (Chike 1993; Choi 2011). Consideration of the unknown peak area was particularly vital for samples with low conversions, which had large epoxide peak areas that covered up the unknown peak area. Such behavior is illustrated by a zero cure sample FTIR curve in Figure 6-13.

To begin, a fully cured sample was created and scanned. A fully cured sample had no peak at 4530 cm^{-1}, allowing the complete area of the unknown peak to be calculated. The measured unknown peak area (which proved no relationship to conversion) from the fully cured sample was subtracted from all epoxide peak areas of other samples. To induce a conversion of 1.0, samples were placed in an oven at 50°C for one hour, 80°C for two hours, and 125°C for three hours.

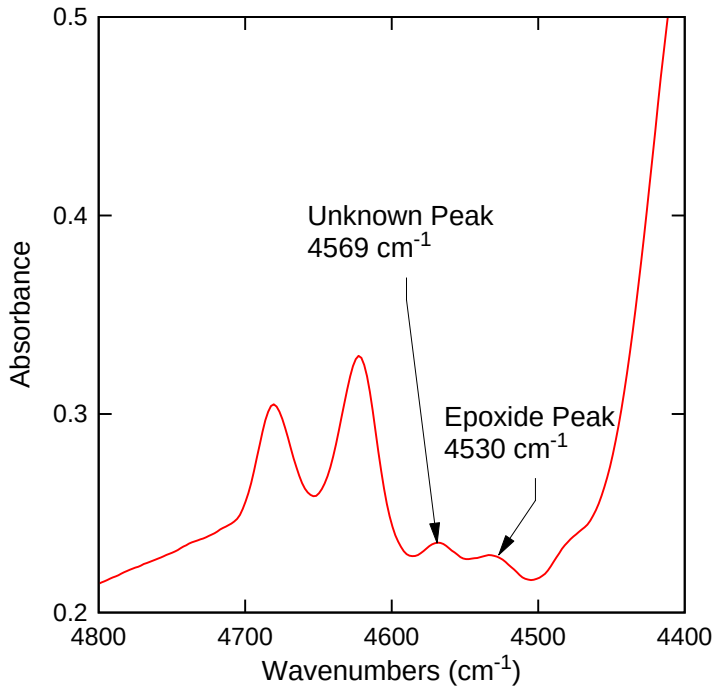

Figure 6-12. Overlapping unknown and epoxide peaks.

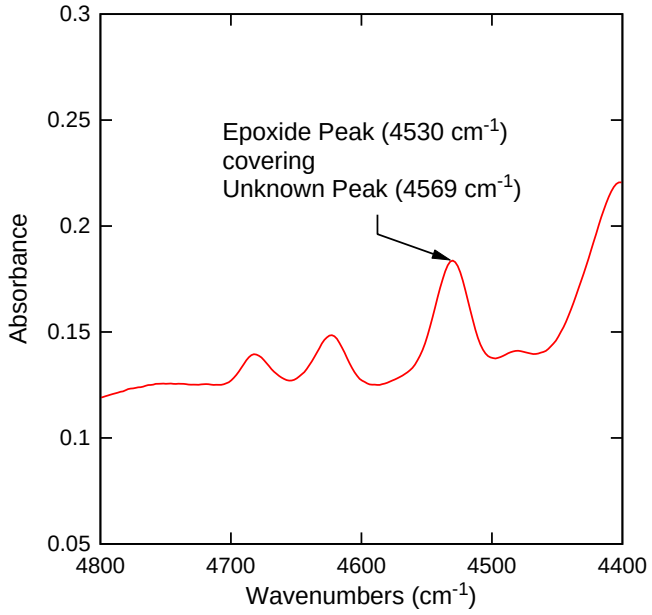

Figure 6-13. Epoxide peak of zero cure sample covering up unknown peak.

Figure 6-14 presents the area calculation of the unknown peak for a fully cured sample. Clicking on the area tool in OMNIC software and then on the peak automatically produces two vertical lines for user controlled boundaries and a user controlled baseline tangent to the curve on either side of the peak. The baseline was adjusted to the lowest slopes on either side of the peak to capture the entire peak area. The vertical lines were then matched to these baseline tangent points demonstrated in Figure 6-14.

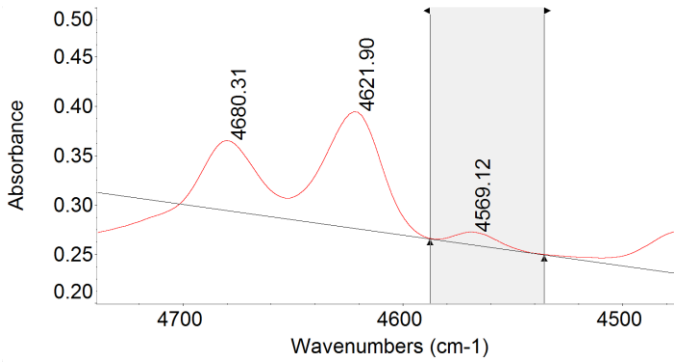

Figure 6-14. Unknown peak area calculation on a 100% cured sample.

All areas calculated from the FTIR curve had to be normalized to account for varied film thicknesses between samples. Thicker samples absorb more light than thinner ones and therefore exhibited larger areas at the peaks of interest. Without normalizing each area, accurate comparisons between samples would not be possible. To normalize areas the phenyl peak (labeled in Figure 6-4) area at 4622 cm^{-1}, which was consistent throughout sample life regardless of conversion, was calculated for each sample. All areas used in calculation of conversion (α) were divided by their respective phenyl peak area of their same FTIR curve. Normalized areas of different samples could then be accurately compared.

Therefore, after calculation of the unknown peak area, the phenyl peak area of the fully cured sample was measured in the same manner as detailed above. The unknown peak area was then divided by the phenyl peak area resulting in a normalized unknown peak area. Next a zero cure sample was created and scanned to establish A(0), providing the largest relative amount of epoxide a sample could contain. First the entire area of both the epoxide peak and the covered unknown peak were measured (Figure 6-15).

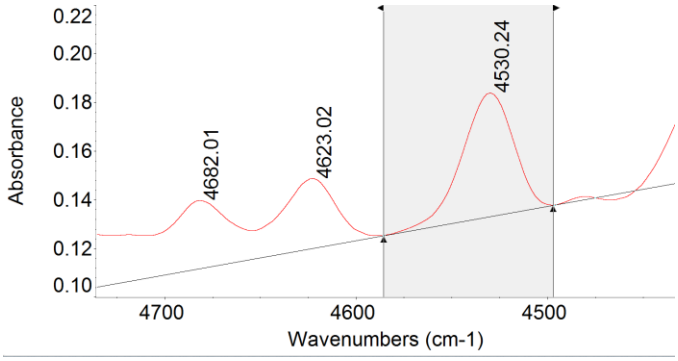

Figure 6-15. Calculation of the epoxide and unknown peak areas of a zero cure sample.

Phenyl peak area for this sample was then calculated for normalization. The previously calculated normalized unknown area for the same epoxy type was subtracted from the normalized epoxide and unknown peak area to provide A(0) the normalized epoxide area for a zero cure sample. This process was conducted once for epoxies A, B, C, and D. Table 6-1 provides an numerical example for calculation of A(0). Note from left to right, each column represents the result of one mathematical step as detailed above.

Table 6-1. Calculation of A(0) for Epoxy A.

Sample Type	Unknown Peak Area	Phenyl Peak Area	Norm. Unknown Peak Area	Sample Type	Epoxide and Unknown Peak Area	Phenyl Peak Area	Norm. Epoxide and Unknown Peak Area	Norm. Epoxide Peak Area Only: A(0)
Fully Cure	0.25	3.45	(0.25/3.45)= 0.072	Zero Cure	1.93	0.75	(1.93/0.75)= 2.57	(2.57-0.072)= 2.5

The calculation of A(t), the amount of epoxide peak area in a partially cured specimen, followed the same steps as A(0) calculation. With the normalized unknown peak area already determined (only one measurement required for each epoxy type) the next FTIR scan needed was of the partially cured sample of which conversion (α) was desired. Area calculation of the unknown and epoxide peak area is detailed in Figure 6-16.

Once this area was normalized with the phenyl peak area of the same curve, the previously calculated normalized unknown peak area was subtracted to provide A(t). An example numerical calculation of A(t) is provided in Table 6-2. With both A(0) and A(t) measured, conversion (α) of the partially cured specimen could be equated. For the

examples provided in Table 6-1 and Table 6-2, conversion would be equal to [1 - (0.116/2.5)]; giving α to be 0.954.

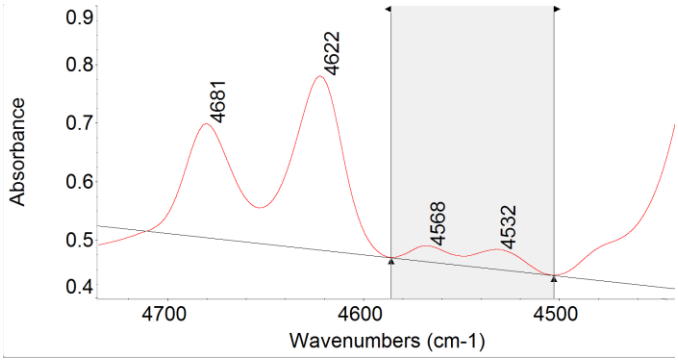

Figure 6-16. Area calculation of the unknown and epoxide peak for a partially cured specimen.

Table 6-2. Example calculation of A(t) for Epoxy A.

Sample Type	Normalized Unknown Peak Area (Table 6-1)	Sample Type	Unknown and Epoxide Peak Area	Phenyl Peak Area	Normalized Unknown and Epoxide Peak Area	Normalized Epoxide Peak Area Only: A(t)
Fully Cure	0.072	Partially Cure	0.47	2.5	(0.47/2.5)= 0.188	(0.188-0.072)= 0.116

Characteristic Water Content

Relative amount of water within samples was calculated in a similar fashion as conversion. The characteristic water peak area at 5230 cm^{-1} provides an indirect measure of the relative amount of water in the sample. This analysis provided a means to track relative amounts of water absorbed into the epoxy during exposure. Unlike conversion analysis that incorporated lower and upper bound limits (0.0-1.0), the water peak area was measured, normalized and simply compared to other samples to track variations in specimen water content.

The characteristic water peak did not overlap other peaks and could be calculated directly for each sample. First, area of the water peak for a specimen of

interest was measured (Figure 6-17). Consistent with the conversion calculation, the phenyl peak area of the corresponding scan was measured and applied to normalize the water peak area. Normalized water peak areas could then be compared to that of other samples. Table 6-3 presents an example of water peak area calculation. Calculated water peak areas will be referred to as characteristic water content in the FTIR results chapter.

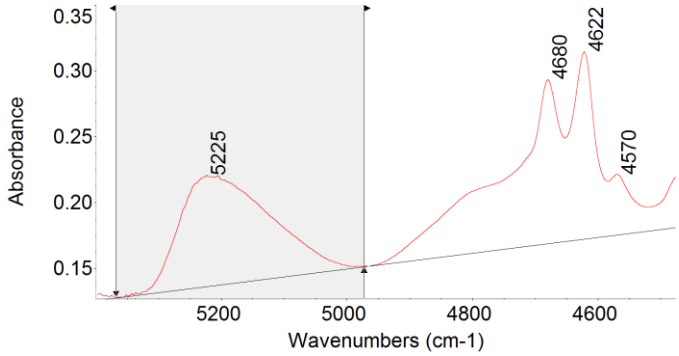

Figure 6-17. Area measurement of characteristic water peak.

Table 6-3. Example calculation of normalized water peak area.

Sample Type	Water Peak Area	Phenyl Peak Area	Normalized Water Peak Area
Any of interest	14.01	2.28	(14.01/2.28)= 6.14

CHAPTER 7
FTIR RESULTS

This chapter presents the FTIR results of epoxies designed for wet layup applications (epoxies A, B, C and D). FTIR data was analyzed to calculate specimen conversion and water absorption. Epoxies E and F, which are typically utilized for near surface mounted applications, were too dense to be cured into films thin enough to transmit light and were not tested in the FTIR. Tracking conversion and water absorption over the course of exposure provided valuable insight into Tg fluctuations of resin epoxies.

Conversion

FTIR analysis of epoxy A, B, C, and D conversions are summarized in Figure 7-1. Data from other research is included in grey where applicable (Choi 2011).

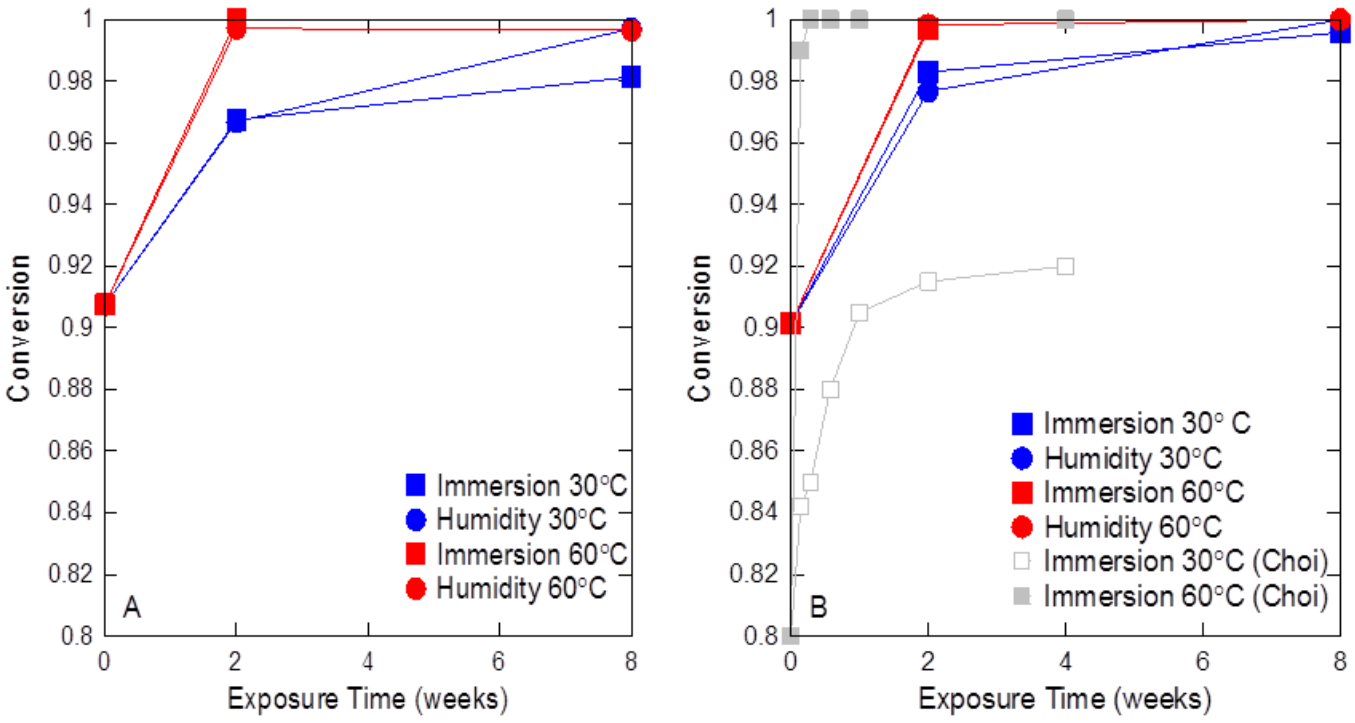

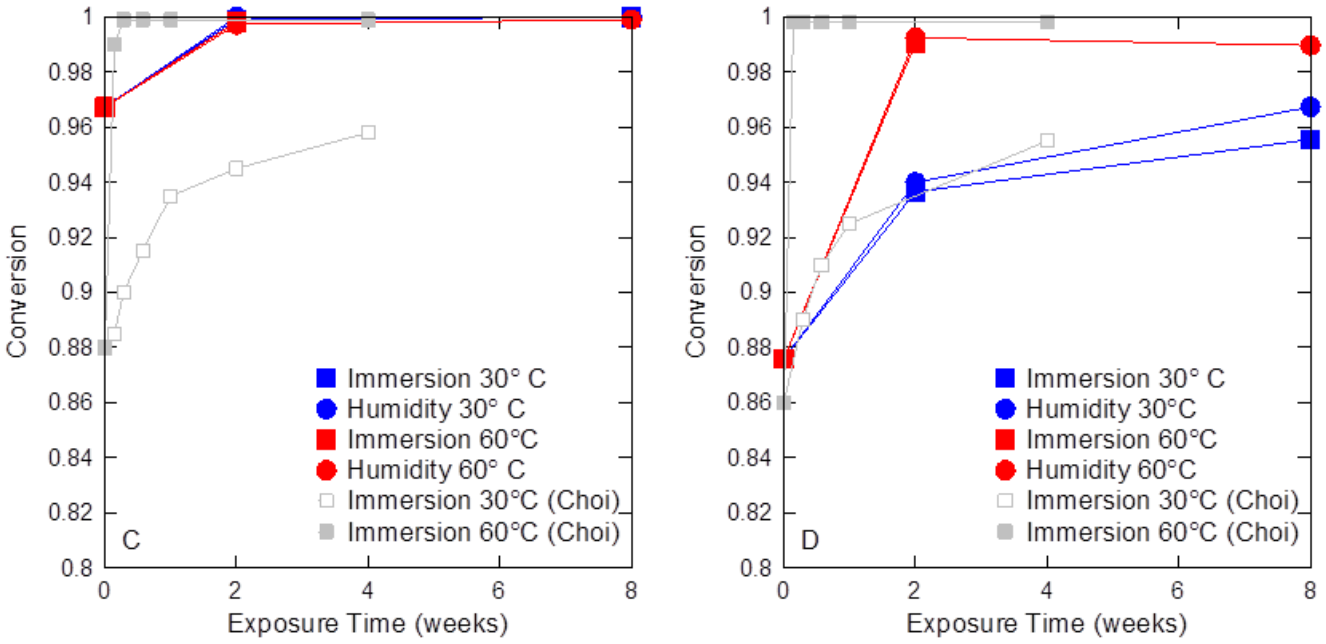

Figure 7-1. Conversion results from FTIR data. A) Epoxy A. B) Epoxy B (includes Choi 2011). C) Epoxy C (includes Choi 2011). D) Epoxy D (includes Choi 2011).

The plots indicate increases in cure throughout the eight week exposure period despite variations in moisture and temperature conditioning. These results were generally expected since the epoxy samples were cured under laboratory conditions (20-24°C) which was 6 to 40ºC cooler than temperatures experienced during exposure (30 and 60ºC). There is a very small negative slope between 2 and 8 weeks in plots A and D for 60°C samples. For example, plot D changes from 0.995 to 0.99 conversion, this 0.5% difference is data noise. It is only possible to reduce the amount of crosslinking by burning the epoxy structure, which is not occurring during conditioning (Douglas 2013).

Closer inspection of Figure 7-1 reveals 60°C samples (red) consistently had a larger plots A, B, and D) or equal (plot C) values of conversion compared to 30°C samples (blue) at each exposure time tested. Such behavior demonstrates the major influence that temperature had on the conversion value of samples. Another clear

observation is the greater slope of conversion increase exhibited by the 60°C samples between zero and two weeks of exposure compared to the 30°C samples. For example, epoxy A 60ºC specimen conversions increased by 0.0925 from zero to two weeks of exposure while 30ºC specimens only increased by 0.0593. Once samples reached a conversion value near the maximum of 1.0, it was maintained for the remaining exposure.

Exposure temperature, above that experienced during the initial cure, functioned as a catalyst for cross-linking within the epoxy structure, thereby increasing conversion. In addition, if exposure temperature was above the Tg, then the epoxy transitioned from a glassy to a rubbery state. This transition allowed additional cross-linking opportunities to become available between polymer chains that were not accessible in the glassy state. At the time of initial exposure, 60°C was greater than the Tg of all epoxies tested, therefore all 60°C samples reached a conversion of 1.0 much sooner than 30°C samples as Figure 7-1 indicates.

Epoxies A, B, and D had similar conversion values prior to exposure ranging from 0.88 to 0.91. Epoxy C, however, had a larger control conversion of 0.96. In addition, epoxy C under 30°C conditioning reached a conversion of 1.0 after only two weeks of exposure while equivalent samples of the other epoxies took at least eight weeks. Although epoxy C 30°C samples reached 1.0 sooner than the others, does not mean it increased at a faster rate than the others. Epoxies A, B, and D did increase by 0.05-0.08 from their respective control conversion after two weeks of exposure. Because epoxy C 30ºC samples already started at a conversion of 0.96 they only had to increase by 0.04 to reach 1.0. This observation suggests that the conversion of the

epoxy prior to exposure influenced how quickly the sample fully cured during exposure. Interpretation of cure behavior in Figure 7-1C also indicates that epoxy C cures at lower temperatures than epoxies A, B, and D.

Conversion data for immersed samples (square points) and humidity samples (circular points) were very similar, as Figure 7-1 illustrates. This behavior was expected since conversion is directional proportional to temperature and is unrelated to the degree of water saturation. This behavior was consistent for both 30°C and 60°C environments for all epoxy types.

Conversion data from previous research for epoxies B, C, and D were plotted in grey (Choi 2011) and provided conversion values for shorter exposure periods than exercised in the present research. Grey data in Figure 7-1 B, C, and D reveal that all 60ºC samples reached a conversion value near 1.0 after only two days of exposure. This trend agrees well with new research (red), regardless of whether samples were immersed or exposed to humidity.

Hollow grey points, indicating 30ºC immersion sample data from prior research, plateaued to lower conversions for epoxies B and C than the new blue data as displayed in Figure 7-1B and C. Conversely, epoxy D 30ºC data from both sets of research matched very well (Figure 7-1D). Equally important to note, is the 0.09-0.1 difference in control sample conversions between prior and new data for epoxies b and c, while epoxy d only exhibited a 0.015 difference.

Differences between control conversions likely resulted from differences in curing conditions between new and previous research. Samples from previous research were stated to have cured under ambient conditions, suggesting a constant 20ºC room

temperature (Choi 2011). In the present research, samples were cured at laboratory temperatures, which proved to range from 20ºC to 25ºC during the cure period. This potential difference in curing temperature would explain the 1.5-10% increase of control sample conversions.

Interestingly, data from epoxy D 30°C samples had both the closest control conversion and plateau behavior between new and prior research. Although epoxies B and C plateaued to higher conversions than that of prior research, they did increase from the control conversion at a similar rate. For example, 30°C epoxy B samples increased 0.085 over two weeks in this research while prior research epoxy B samples increased 0.115. Both characteristics infer that conversion will increase at a similar rate despite the initial conversion value at the beginning of exposure, but will only incite a finite amount of conversion change for a given exposure temperature. Therefore, because new 30°C samples of epoxies B and C started out at a higher conversion than previous research, they increased and plateaued to a larger conversion as well.

By calculating specimen conversions, each Tg could be compared to that of an unexposed specimen of the equal conversion. Because conversion and plasticization have proven to be the two main influences on Tg fluctuations, knowledge of the conversion of exposed samples allowed the plasticization effect on Tg to be isolated.

Water Absorption

Water absorption of specimens was tracked by measuring characteristic water content from FTIR data. FTIR analysis of epoxy A, B, C, and D characteristic water contents are summarized in Figure 7-2. Data from other research is included in grey where applicable (Choi 2011).

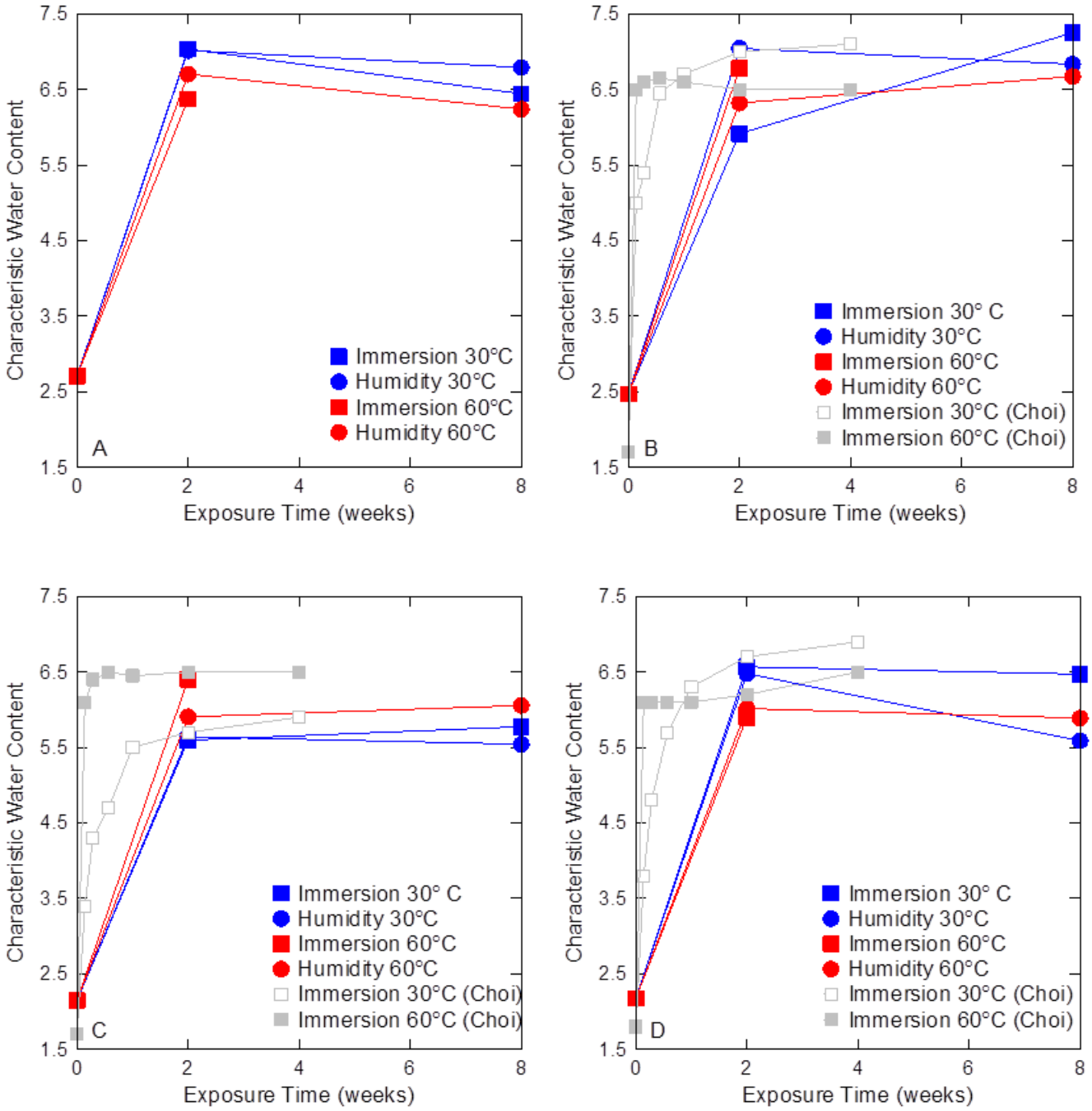

Figure 7-2. Water absorption results from FTIR data. A) Epoxy A. B) Epoxy B (includes Choi 2011). C) Epoxy C (includes Choi 2011). D) Epoxy D (includes Choi 2011).

All samples exhibited an increase in characteristic water content during exposure as

Figure 7-2 denotes. It appears that specimens reached a relatively common fully

saturated state despite epoxy type, after two weeks of exposure and was generally maintained for the remainder of exposure.

Data from Figure 7-2 illustrated no apparent difference in water absorption of immersed samples (square points) and those exposed to 100%RH (circular points). This suggests that by two weeks of exposure, 100%RH samples had already reached full saturation and were equal in water content to immersed samples. Water content also appears to be independent of exposure temperature by two weeks of exposure for all epoxy types.

Epoxy A, B, C, and D specimens all started exposure with 2 - 2.5 characteristic water content and plateaued to 5.5 – 7 over the eight week exposure period. Exposed samples on average had characteristic water content 2.68 times larger than that of their equivalent control samples. Epoxy A did present a slight decrease in water content of to 8.4% between 2 week and 8 week samples. This behavior was unexpected and the cause is not clear.

Water content data from prior research was included as grey points in Figure 7-2 to illustrate water absorption behavior between zero and two weeks of conditioning (Choi 2011). It is clear that during the first week of exposure, water was absorbed faster into 60ºC samples (solid grey points) compared to 30ºC samples (hollow grey points). Full saturation was achieved within 1-4 days of exposure in 60ºC conditions and not until about 2 weeks in 30ºC conditions. Higher exposure temperatures provide more energy to water molecules, thereby increasing water diffusion into the epoxy network explaining the quicker saturation of 60ºC samples verses 30ºC samples. With extended

exposure, that beyond 2 weeks, temperature was not related to the amount of water contained in samples.

Water content of each sample was measured to investigate the rate of epoxy water absorption, as well as to analyze possible correlations between Tg reduction and plasticization. Because full saturation was maintained for majority of the 8 week exposure period, effects of plasticization are predicted to be relatively constant. Other effects on Tg caused by water could potentially be influenced by Type II bound water (Zhou 1999).

Master Plots

Because Tg fluctuations during hygrothermal exposure are dependent on two different competing influences (added cure and plasticization), master plots were developed to isolate Tg fluctuations caused by plasticization only. Master plots graph Tg vs conversion and included a theoretical curve that indicates what Tg value is associated for a given, unexposed sample conversion. With these theoretical curves, the Tg of exposed samples could be compared to that of unexposed samples of equal conversion. By plotting Tg based on sample conversion, the effects of added cure are neutralized, leaving any differences in Tg to be the result of plasticization (Choi 2011).

Theoretical curves were created implementing Equation 7-1.

$$Tg = \frac{(1-\alpha)Tg_0 + \alpha\left(\frac{\Delta C_{p\infty}}{\Delta C_{p0}}\right)Tg_\infty}{(1-\alpha) + (\frac{\Delta C_{p\infty}}{\Delta C_{p0}})\alpha} \qquad \text{Equation 7-1}$$

Where α is conversion (0 to 1.0), Tg0 and ΔCp0 are associated with a 0% cured sample and Tg∞ and ΔCp∞ are derived from a 100% cured sample. ΔCp is the change in heat capacity before and after the glass transition. This semi empirical equation was

developed from research by Couchman and Karasz (1978) to describe the relationship between Tg and cross-linking (conversion) in polymers.

To create theoretical curves unexposed samples are cured to various conversions, and must include 0.0 and 1.0 to derive Tg0 and Tg∞. Other unexposed data between 0.0 and 1.0 conversion values are plotted to fit the theoretical curve generated by Equation 7-1. With Tg0 and Tg∞ known, ΔCp∞/ΔCp0 was adjusted match the theoretical curve to the unexposed data as best as visually possible. Once the theoretical curve accurately depicted the Tg and conversion relationship, exposed data were plotted to assess the influence of plasticization on Tg.

An example master plot from a prior study is presented in Figure 7-3 (Choi 2011). All unexposed sample data are identified by black diamonds and were used to fit the theoretical curve (red line).In Figure 7-3, blue points represent 30°C immersed samples, green represent 40°C, pink points represent 50°C and red points represent 60°C. All data were recorded over a period of four weeks. As pictured, all exposed samples had a Tg less than the theoretical curve. This reduction in Tg is a result of the influence of the moisture on the Tg.

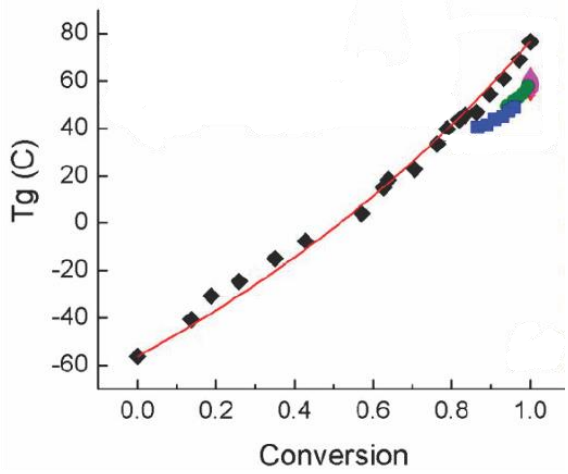

Figure 7-3. Example master plot for epoxy D (Choi 2011).

Because the conversion was near 1.0 for most of the samples in this research, the area of interest was very narrow. Consequently, it was only necessary to use three control points to fit the theoretical unexposed conversion curve. One control point between 0.0 and 1.0 conversion in addition to 0.0 and 1.0 points as displayed in Figure 7-4 were exercised. Parameters calculated to create theoretical curves for epoxies A, B, C, and D are listed in Table 7-1. Figure 7-5 presents the master plots for epoxies A, B, C and D with the focus between 0.85 and 1.0 conversion values to enhance the view of exposed data.

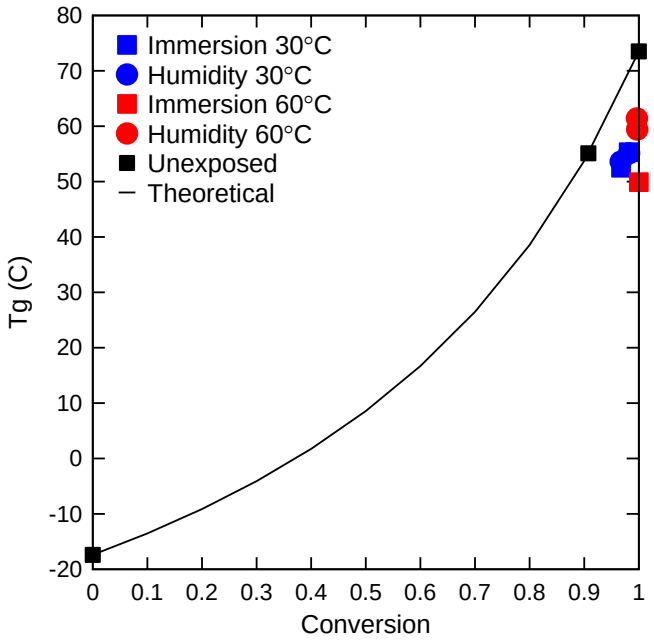

Figure 7-4. Master plot construction for epoxy A.

Table 7-1. Parameters calculated to develop theoretical curves.

Epoxy	Tg_0 (°C)	Tg_∞ (°C)	$\Delta Cp_\infty/\Delta Cp_0$
A	-17.4	73.5	0.40
B	-45.9	72.2	0.68
C	-34.4	71.0	0.29
D	-56.2	76.7	0.69

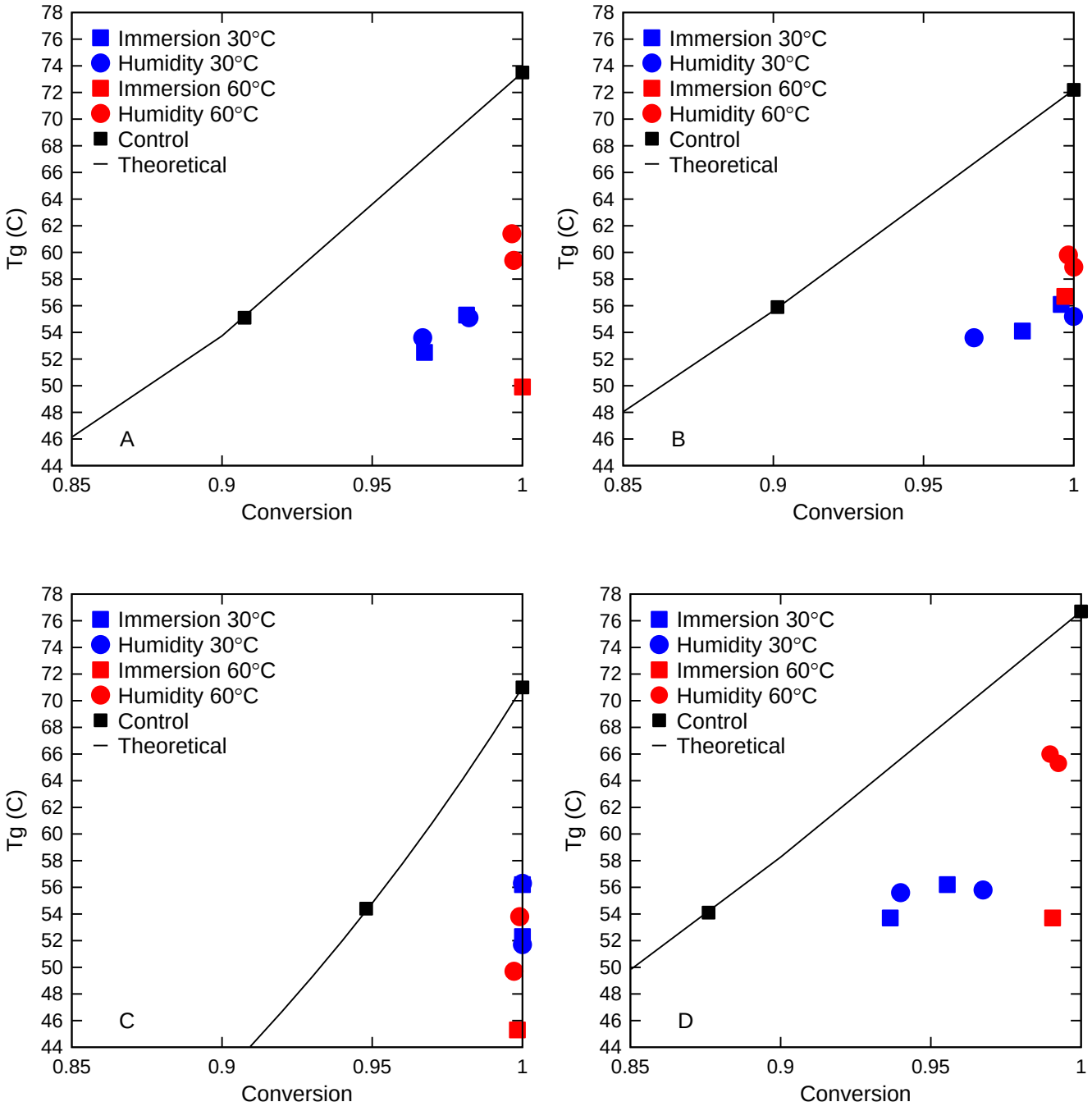

Figure 7-5. Master plots. A) Epoxy A. B) Epoxy B. C) Epoxy C. D) Epoxy D.

Figure 7-5 illustrates Tg reductions of exposed samples from their respective theoretical curves, thus indicating the effects of plasticization. There appears to be little difference between the Tg of 30ºC immersion and humidity samples, as the plots of

Figure 7-5 depict only 0 to 2°C differences. Conversely, 60ºC immersion and humidity samples exhibit similar amounts of conversion, yet the immersion samples (square points) have a Tg consistently lower than humidity samples (circular points); a tendency shared by all epoxies analyzed in this manner, ranging from 3 to12.5°C less.

Recall from Table 3-3, that only one two week 60ºC immersion sample was tested in the FTIR for each epoxy type while a two week and an eight week 60ºC humidity sample was tested. Observing Figure 8-1 and Figure 8-4, it appears that for all epoxy types, 60ºC immersed samples after two weeks of exposure acquired the largest Tg reduction of all sample types. Beyond two weeks, the Tg of these samples did recover slightly as illustrated in Figure 8-1 and Figure 8-4 perhaps due to theorized type II bond water (Zhou and Lucas1999). After this rebound, immersion and humidity 60ºC samples had very comparable Tg values. Thus, if additional 60ºC immersion samples (beyond two weeks of exposure) were included in the master plots of Figure 7-5, humidity and immersed samples would likely demonstrate a more similar behavior.

The lower Tg of two week 60ºC immersion samples suggests that they would contain more water than comparative humidity samples. Illustrated in water absorption plots of Figure 7-2, this is not the case. Therefore with similar amounts of conversion and water absorption, 60ºC immersion samples had larger decreases in Tg than humidity samples after two weeks (see Figure 8-1 and Figure 8-4). This observation indicates that tracking water absorption with the FTIR may not be directly proportional to plasticization or perhaps another effect besides plasticization decreasing Tg exists.

Tg and Characteristic Water Content

Figure 7-6 presents the relationship between Tg reduction and characteristic water content. Tg reduction was calculated for each sample by subtracting the

experimental Tg following exposure from the theoretical Tg of equal conversion. For example, if sample “x” had an experimental Tg of 55ºC and a conversion of 0.95, then α=0.95 was inserted into Equation 7-1 (respective to Table 7-1) to compute a theoretical Tg. If the theoretical Tg was 70ºC in this case, then the Tg reduction would be 15ºC. Tg reduction is represented by ∆Tg in Figure 7-6. Factor of increase in characteristic water content (labeled CWC Ratio in Figure 7-6) for each sample was computed by dividing the water content of the exposed sample by the water content of the respective control sample.

Little if any correlation exists between ∆Tg and increase in water absorption according to the plots in Figure 7-6 (perhaps with the exception of epoxy C). According to Figure 7-2 above, the amounts of water absorbed plateau after two weeks of exposure; therefore very little difference in water content exists amongst data in Figure 7-6 as demonstrated by the narrow ranges of the x axes. The lack of correlation between ∆Tg and water absorption may be explained by the durations of exposure at which testing occurred. By two weeks (the shortest duration tested) samples were already fully saturated (see Figure 7-2); therefore there were little differences in water content beyond two weeks. If shorter durations were tested, for example within the first 48 hours, the variation in water content would be larger and perhaps present a better relationship with Tg reduction.

As noted above, 60ºC immersion samples (red squares) suffer the largest Tg reduction compared to all other sample types, despite sharing similar levels of water content. This suggests that plasticization may be effected by something besides water content as measured with the FTIR or perhaps Tg values reduced due to other means.

All other sample types appear to be hover in a common +/- 5 to 15ºC Tg range and share similar water contents, which likely was due to all samples reaching full saturation.

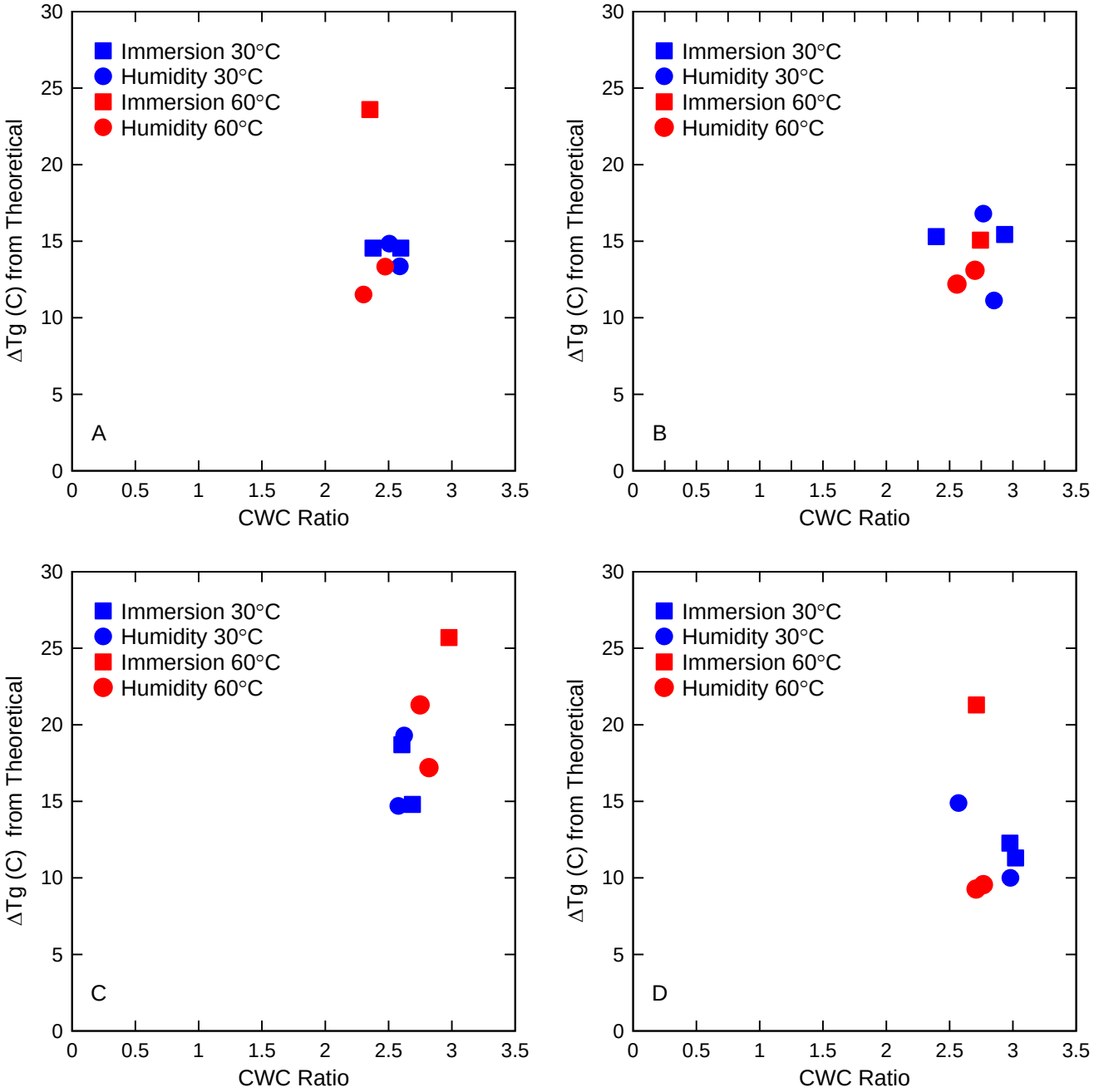

Figure 7-6. Tg reduction in relation to increases in sample water content. A) Epoxy A. B) Epoxy B. C) Epoxy C. D) Epoxy D.

By combining all ΔTg data for epoxies A, B, C and D in Figure 7-7, some relationships are revealed. Most pronounced is that water absorption beyond that of the control samples was associated with increases in ΔTg. Also, the 60ºC humidity samples (red circle data points) were the only exposure condition to model a direct relationship between water absorption and ΔTg. Conversely, all other exposure conditions portrayed an unrelated, scattered relationship within the 5.6-7.3 range of characteristic water area. Interestingly, although two week 60ºC immersion samples (red squares) had similar amounts of water absorbance as other conditions, they generally displayed the largest reduction in Tg in Figure 7-7.

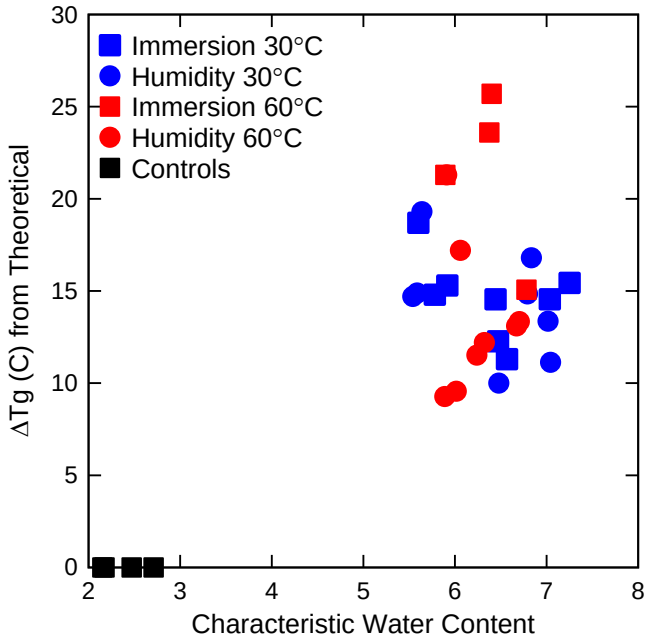

Figure 7-7. Changes in Tg for epoxies.

CHAPTER 8
DSC RESULTS

DSC data allowed the Tg of six different epoxies to be tracked over 12 weeks of exposure. Some epoxies shared comparable shifts in Tg, while others behaved uniquely. Below, observed characteristics are presented and summarized.

Clear Resins

Clear resin epoxies A, B and D all shared similar Tg fluctuation behavior over the 12 week exposure. Figure 8-1 summarizes these fluctuations. Temperature of exposure proved to have a strong influence on the Tg of clear resin epoxies A, B, and D. By 12 weeks, all samples exposed to 60ºC temperatures had a Tg greater than their equivalent (same epoxy and moisture condition) 30ºC sample as illustrated in Figure 8-1.

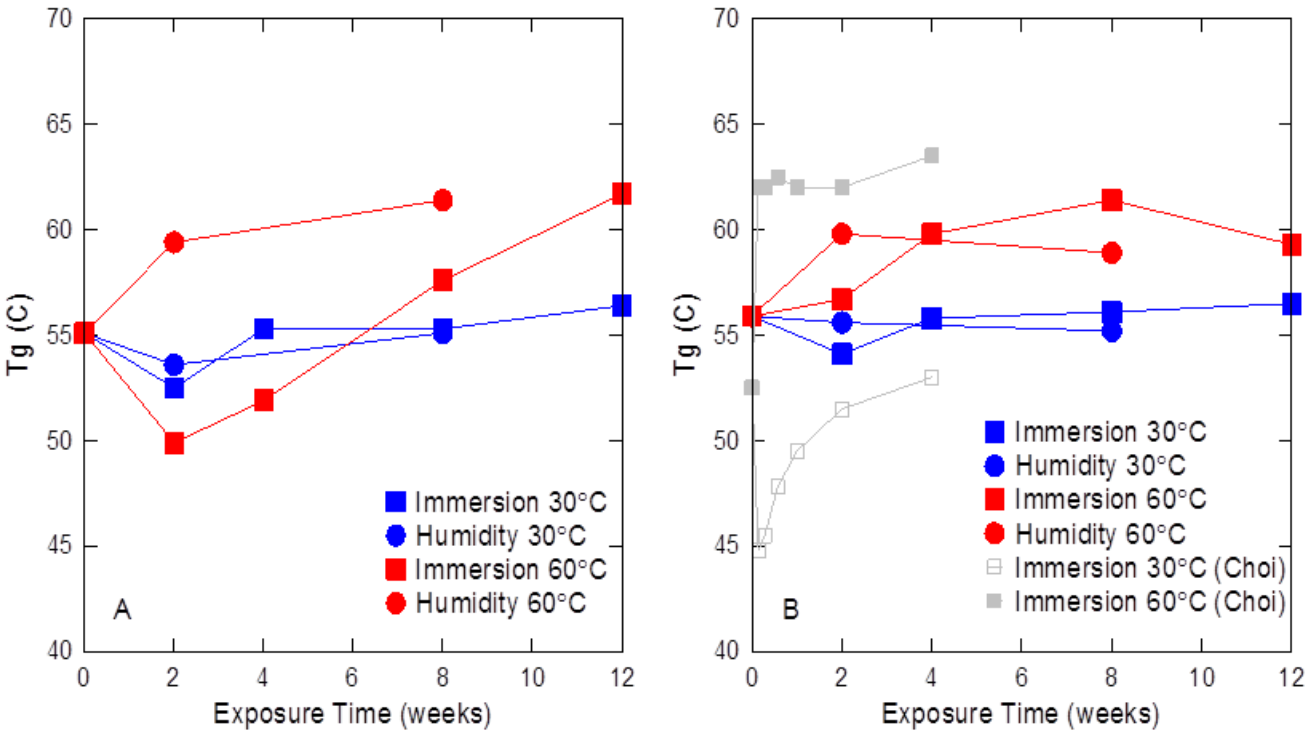

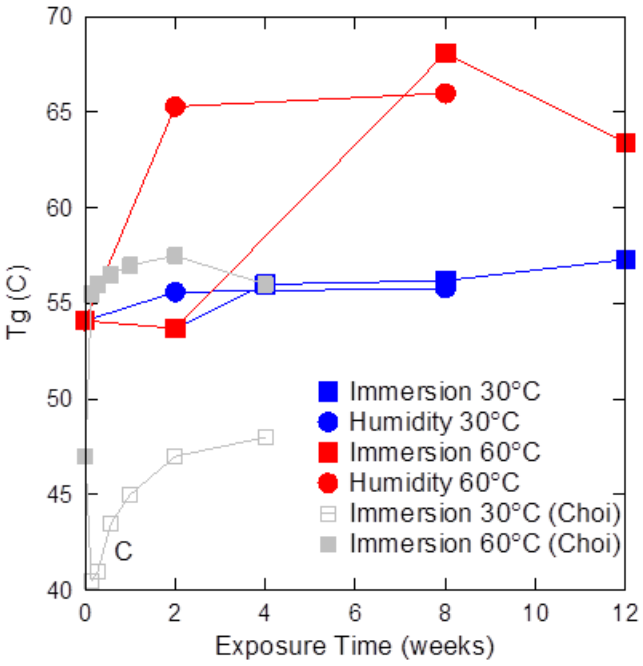

Figure 8-1. Tg fluctuation over 12 weeks of exposure. A) Epoxy A. B) Epoxy B (includes Choi 2011). C) Epoxy D (includes Choi 2011).

This behavior occurred at 8 and 12 weeks despite the type of moisture conditioning, as both 60º C immersed and humidity samples produced Tg values larger than all 30ºC equivalent samples. By the end of the 12 week exposure, the final Tg was greater than the original control Tg (prior to exposure) for all exposure conditions.

Conversion plots (Figure 7-1) and water absorption plots above (Figure 7-2) of epoxies A, B, and D provided explanation of the Tg plots above. Although the water absorption levels were very close between 30ºC and 60ºC samples, the conversion of 30ºC samples for these epoxies did not quite reach 100% such as the 60ºC samples. Consequently, 60ºC specimens had a denser cross-linked structure explaining their larger Tg at the end of the 12 week period.

A unique characteristic of epoxy A Tg behavior is the steady increase in Tg between 2 and 12 weeks of exposure. Observation of Figure 7-1 suggests that by 2

weeks conversion has already plateaued. Therefore, increases in Tg beyond this point stem curiosity. Studying Figure 7-2 it can be noted that the water content of all exposure types of epoxy A specimens slightly decreased between 2 and 8 weeks. Although what caused this decrease is not fully understood, it could potentially explain why the Tg increased in epoxy A samples after 2 weeks despite already reaching nearly a conversion of 1.0. Tg increase beyond 2 weeks could also be related to Type II bond water as proposed by Zhou and Lucas.

Figure 8-1 also gives evidence that samples exposed to humidity were not affected by plasticization during the first 2 weeks of exposure as much as immersed samples. Looking at each type of the clear resin epoxy, every 2 week humidity sample had a Tg higher than their respective immersed sample. In Figure 8-2 it is clear that plasticization had a stronger effect on immersed samples (red) than it did on humidity samples (blue).

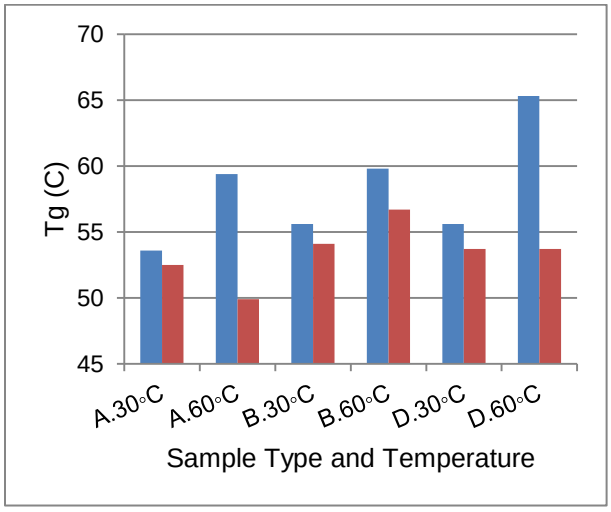

Figure 8-2. Tg of 2 week exposed samples of clear resin epoxies; blue represents humidity samples and red presents immersed samples.

Although there were some large differences in Tg between immersed and humidity samples after 2 weeks of exposure, these differences seemed to decrease as

exposure continued. By 12 weeks the difference in Tg between humidity and immersed samples reduced to less than +/- 3ºC as presented in Figure 8-3. This is most likely due the slight Tg recovery of immersed samples over the course of the exposure. Figure 8-3 provides evidence that the longer 100%RH samples are exposed the more they exhibit glass transition temperatures similar or equal to that of immersion samples.

Interestingly, water absorption plots for epoxies A, B, and D (Figure 7-2) do not display much difference in water content between humidity and immersion samples after 2 weeks of exposure. Yet 60°C immersed samples suffer a larger Tg reduction than 60°C humidity samples at 2 weeks. This suggests that water content measured may not be as proportionally related to effects of plasticization on the Tg as previously thought or Tg reduction may be dependent on additional factors besides water content such as temperature and moisture conditioning.

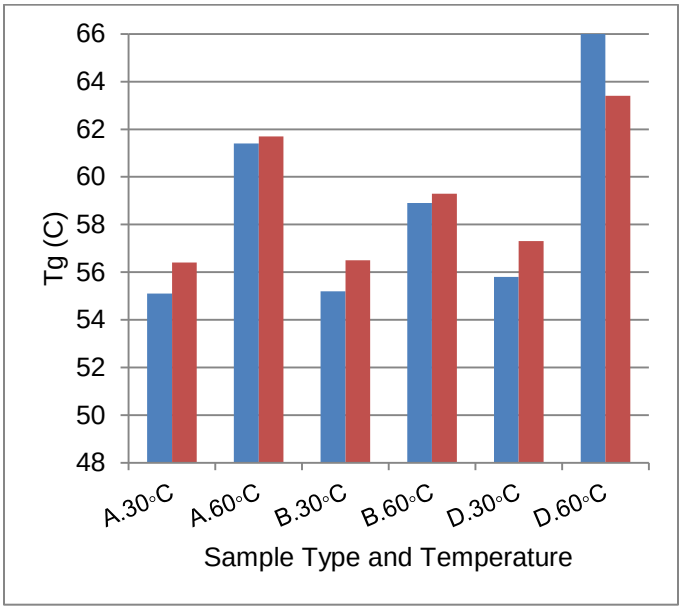

Figure 8-3. Tg of 8 week humidity samples and 12 week immersed samples.

Non-Clear or Non-Resin Epoxies

The non-clear resin (epoxy C) and the paste epoxies (E and F) each exhibited unique Tg behavior. Epoxy C Tg behavior appeared to be dominated by plasticization over the entire exposure period as illustrated in Figure 8-4.

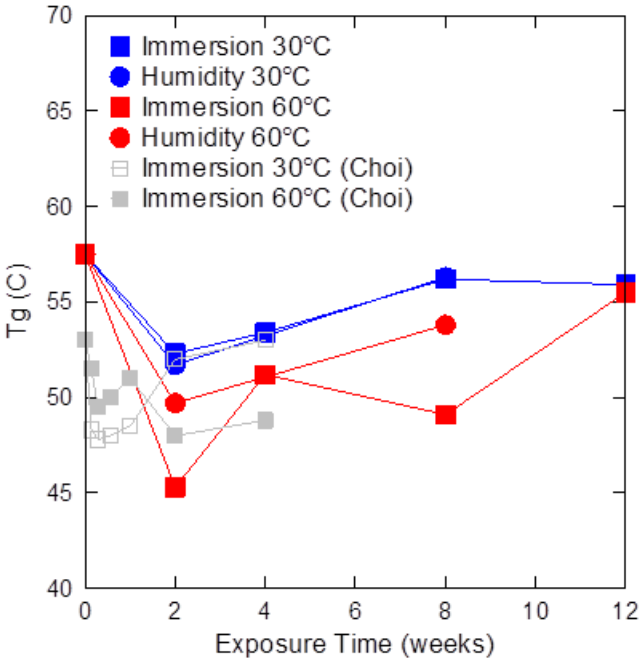

Figure 8-4. Epoxy C Tg changes (includes Choi 2011).

After 12 weeks, the Tg failed to rebound to its control Tg temperature that existed prior to exposure, despite additional cross-linking as Figure 7-1C illustrates. The largest decrease in Tg temperature was 13º C following exposure in 60º C water for 2 weeks. All epoxy C samples had their lowest Tg after 2 weeks of exposure despite conditioning type, followed by a slight recovery over time as observed in Figure 8-4.

The Tg may not have rebounded to the control value because the control sample already had a conversion of 0.96 prior to exposure according to Figure 7-1C. Therefore, added cure would increase Tg less than that of a 0.85 conversion sample (such as the controls of other epoxies). Because added cure was limited, plasticization proved to be

the controlling factor on Tg, hence, reducing the Tg of exposed samples consistently below the control Tg.

Epoxy F exhibited the largest change in Tg of all the epoxy systems, with a drop of 19º C under water immersion conditions, as depicted in Figure 8-5.

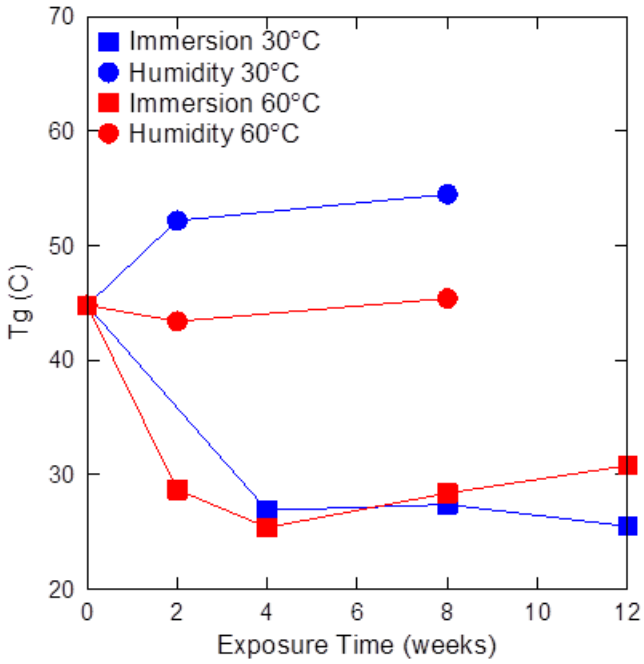

Figure 8-5. Epoxy F Tg changes.

Apparent from Figure 8-5, epoxy F immersed samples were very sensitive to plasticization, as each displayed a large drop in Tg that never recovered over 12 weeks of exposure. This large drop in Tg is interesting when compared to the Tg of epoxy F humidity samples which stayed close to or increased above the control Tg. This data suggested that there was a much more plasticization occurring in immersed samples than in the humidity samples. Unfortunately paste epoxies were unable to be analyzed in the FTIR, therefore the water content of epoxy F samples were not measured.

Unlike the other epoxy systems, epoxy E demonstrated sporadic behavior at 2 weeks exposure (see Figure 8-6).

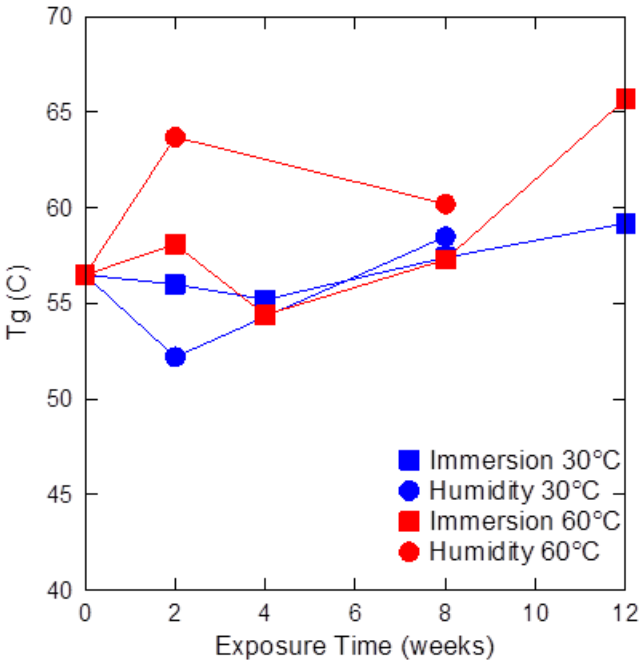

Figure 8-6. Epoxy E changes.

The epoxy E 2 week 60º C samples yielded a higher Tg than the 30º C samples, and was the only epoxy to show this behavior for both water immersion and humidity. By 8 weeks, samples of all exposure types converged to Tg temperatures slightly above (+0.5 to +3.5^{o}) the control Tg temperature. Therefore, over time the competitive effects of added cure and plasticization neutralized with extended exposure beyond 8 weeks.

Implications of Tg Measurement Method

As previously noted in Chapter 3, glass transition is a region of temperature over which a material transitions from a glassy state to a rubbery state. Because this transition occurs over a region and not at a specific temperature, Tg values are simply an estimate of what temperature the material losses stiffness. Different thermal analysis techniques take different property measurements (tan(δ), modulus, heat flow etc.) and select different points of unique curve behavior (peaks, tangents, step changes etc.) to calculate Tg values. These varied techniques all provide technically correct estimates of

Tg by providing a temperature within the glass transition region, but the Tg of one material will vary between different methods.

This makes it difficult to compare Tg values calculated with the DSC to those calculated by manufacturers who may use the DMA or TMA according to AASHTO and ICC requirements. Even if a manufacturer documents a Tg was calculated with the DMA in accordance ASTM D4065 as required by ICC, it is still difficult to compare to a DSC calculation. This problem stems from ASTM D4065, which does not specify which of the three DMA curves (tan(δ), storage modulus, or storage modulus derivative) Tg should be calculated from as illustrated in Figure 2-4.

Unless the thermal analysis method and curve of Tg calculation is identified, it is unreasonable to compare Tg values from other sources. For example, depending on which curve is chosen to calculate Tg from the DMA, values can be 5 to 15^{o}C larger than a DSC Tg calculation (Wunderlich 2005). For this reason, it is not practical to compare Tg values calculated here to those reported by manufacturers in Table 3-1, who either did not report the method of Tg calculation, or did not report the DMA curve selected for Tg calculation.

Regardless of inconsistencies between calculation methods, relative Tg fluctuations due to exposure determined by one method can be fairly compared to that of any other method. For example, if DSC calculated a decrease in Tg of 17^{o}C between 2 and 12 weeks of exposure, the DMA and TMA should measure a decrease of 17^{o}C as well.

CHAPTER 9
SUMMARY AND CONCLUSIONS

Summary

To gain understanding of how exposed epoxy may affect FRP composite bond durability, epoxy was monitored over time under hygrothermal conditions. Tg, conversion, and plasticization of the epoxy were measured, providing understanding of how the epoxy matrix is affected over time from conditioning.

The response of six FRP composite epoxies was monitored following varied exposure conditioning. Tg was calculated with a DSC over the course of a 12 week exposure in either 60°C water immersion, 30°C water immersion, 60°C 100% RH, or 30°C 100% RH. Sample conversion and water content were measured by means of FTIR instrumentation to support Tg data analysis. Conclusions from this work will aid recommendations for acceptable exposure, test, and field conditions for FRP composites that incorporate epoxy systems.

Conclusions

All samples experienced increases in conversion. Conversion increase during exposure was dependent on temperatures experienced during initial cure relative to exposure temperatures. Conversion was independent of moisture conditioning (immersion vs. humidity). Samples were fully saturated by 2 weeks of exposure regardless of exposure temperature or moisture conditioning. Water content of exposed samples increased 2.7 times that of unexposed control samples on average.

In general, during the exposure period, Tg decreased initially with the immersed 60°C 2 week samples consistently demonstrating the largest reduction in Tg of all

sample types. Longer exposures, however, resulted in a net increase in the Tg with 60°C 12 week immersed samples demonstrating the highest Tg values.

Tg fluctuations occurred over the 12 week exposure period despite relatively consistent values of conversion and water absorption. Most sample types (with the exception of epoxy F) experienced a large Tg reduction after 2 weeks followed by slight recovery over the rest of the 12 week exposure. This is most likely due to secondary hydrogen bonding as proposed in prior research (Choi 2011; Zhou and Lucas 1999). The lowest Tg recorded was 25.4°C (epoxy F, 60°C immersion, 4 weeks of exposure).

CHAPTER 10
RECOMMENDATIONS

Epoxy Bond Tests

If bond tests are to be performed to estimate durability of FRP composites for field conditions the accelerated aging parameters should include water immersion for 2 weeks in the maximum design temperature expected in the field. These conditions will produce the largest Tg reduction and a fully saturated state of the epoxy, which together should result in the lowest bond capacity possible in the field.

When using hygrothermal conditioning, the bond sample must be cooled after conditioning to a temperature below its reduced Tg prior to load testing to ensure the epoxy is in a glassy state. Exposure to water will create a plasticized epoxy matrix, resulting in a reduced Tg and glassy state stiffness (Stewart 2012). Degradation of the bond is driven by plasticization of the epoxy concrete interface and the epoxy itself. A plasticized epoxy will demonstrate reduced stiffness and not be able to transfer as much load as samples not exposed to moisture.

Load tests specified by codes or performed by researchers that involve exposing epoxy to water will experience a reduction of epoxy stiffness and Tg. It was found here that some epoxies will experience Tg reductions into normal temperature ranges. For this reason if load testing requires moisture conditioning, then Tg of epoxies involved should be calculated following the same conditioning. This would allow researchers to ensure that the temperature of testing environment is well below the sample Tg. If load tests were performed with no understanding of the epoxy Tg, it is possible that the epoxy would be in a rubbery state during load testing, resulting in very low failure loads.

Field Application

Following hygrothermal conditioning the Tg of epoxy E reduced as low as 25.4^{o}C (77.7^{o}F) and the other epoxies reduced to 45 to 54^{o}C (113^{o}F to129^{o}F). These Tg values are well within the temperature range FRP composites would be exposed to in the field. Therefore, it is evident that cold cure epoxies with Tg values near design temperature conditions should not be installed in areas were water immersion is possible such as the wrapping of bridge piles.

Because Tg reductions due to plasticization are residual any excessive exposure to moisture may be concerning such as areas with frequent rainfall for high humidity averages. For epoxy E, humidity did not cause as large of Tg reductions as immersion did, but for other epoxy types effects of humidity and immersion were similar. Therefore cold cure epoxies are best suited for indoor applications or in relatively dry climates.

LIST OF REFERENCES

Aiello, M., Frigione, M., and Acierno, D. (2002). ”Effects of environmental conditions on performance of polymeric adhesives for restoration of concrete structures.” *J. Mater. Civ. Eng.*, 14(2), 185–189.

American Association of State Highway and Transportation Officials (AASHTO). (2012). “Design of bonded FRP systems for repair and strengthening of concrete bridge elements.” Washington, DC.

AASHTO LRFD Bridge Design Requirements. (2010). “Uniform temperature: Temperature range for procedure B.” *Article 3.12.2.2.* Washington, DC.

American Composites Manufacturers Association. (2013). “In pursuit of the new: FRP protection heats up”. *Composites Manufacturing Online*.

American Concrete Institute (ACI). (2007). “Report for FRP reinforcement for concrete structures.” *Rep. No. 440-07,* Farmington Hills, MI.

ACI. (2008). “Guide for the design and construction of externally bonded FRP systems for strengthening concrete structures.” *Rep. No. 440.2R-08*, Farmington Hills, MI.

American Society of Civil Engineers (ASCE). (2013). “2013 report card for America’s infrastructure”. *www.infrastructurereportcard.org*, Reston, VA.

ASTM (2007). “Standard test method for deflection temperature of plastics under flexural load in the edgewise position.” *ASTM D648-07*, West Conshohocken, Pa.

ASTM (2008). “Standard test method for assignment of the glass transition temperatures by differential scanning calorimetry.” *ASTM E1356*, West Conshohocken, Pa.

ASTM. (2008). “Standard test tethod for resistance of concrete to rapid freezing and thawing.” *ASTM C666 / C666M – 08,* West Conshohocker, Pa.

ASTM. (2009). “Standard test method for assignment of the glass transition temperature by dynamic mechanical analysis.” *ASTM E1640-09*, West Conshohocker, Pa.

ASTM. (2009). “Standard test method for pull-off strength of coatings using portable adhesion testers.” *ASTM D4541-09e1*, West Conshohocker, Pa.

ASTM. (2010). “Standard test method for flatwise tensile strength of sandwich constructions.” *ASTM C297-10*, West Conshohocken, Pa.

ASTM. (2012). “Standard practice for plastics: Dynamic mechanical properties: determination and report of procedures.” *ASTM D4065-12*, West Conshohocken, Pa.

ASTM. (2012). “Standard test method for linear thermal expansion of solid materials by thermomechanical analysis.” *ASTM E831-12*, West Conshohocken, Pa.

ASTM. (2012a). “Standard practice for operating fluorescent ultraviolet (UV) lamp apparatus for exposure of nonmetallic materials.” *ASTM G154-12a*, West Conshohocken, Pa.

Au, C., and Buyukozturk, O. (2006). “Peel and shear fracture characterization of debonding in FRP plated concrete affected by moisture.” *J.of Compos. Constr.,* 10(1), 35-47.

Chike, K. E.; Myrick, M. L.; Lyon, R. E.; Angel, S. M (1993). “Raman and near-infrared studies of an epoxy resin.” *Appl. Spectrosc.* 47(10), 1631-1635.

Choi, S. (2011). “Study of hygrothermal effects and cure kinetics on the structure-property relations of epoxy-amine thermosets: Fundamental analysis and application.” M.E. Thesis, Uni. of Florida, Gainesville, FL.

Couchman, P. R., Karasz, F. E. (1978). “A classical thermodynamic discussion of the effect of composition on glass transistion temperatures.” *Macromolecules* 11(1), 117-119.

Dai, J.; Yokota, H.; Iwanami, M. Kato, E. (2010). “Experimental investigation of the influence of moisture on the bond behavior of FRP to concrete interfaces.” *J.of Compos. Constr.,* 14(6), 834–844.

Djouani, F., Connan, C., Delamar, M., Chehimi, M. M., Benzarti, K. (2011). “Cement paste-epoxy adhesive interactions.” *Constr. Build. Mater.,* 25(2), 411-423.

Dolan, C.W., Tanner, J., Mukai, D., Hamilton, H. R., Douglas, E. (2008). “Design guidelines for durability of bonded CFRP repair/strengthening of concrete beams.” *NCHRP Web-Only Document 155.*

Douglas, E. (2013). “Introduction to materials science and engineering”. *Pearson Higher Education Inc,* Upper Saddle River, NJ.

El-Hacha, Raafat., Green, M., Wight, G. (2010). “Effect of severe environmental exposures on CFRP wrapped concrete columns.” *J.of Compos. Constr.,* 14(1), 83–93.

Florida Climate Center. (2013). “Relative Humidity.” *National Climatic Data Center,* Asheville, NC.

Frigione, M., Aiello, M.A., Naddeo, C. (2006). “Water effects on the bond strength of concrete/concrete adhesive joints.” *Constr. Build. Mater.,* 20, 957-970.

Gartner, A. (2007). “Development of a flexural bond strength test to determine environmental degradation of CFRP composites bonded to concrete.” M.E. Thesis, Uni. of Florida, Gainesville, FL.

Gartner, A., Douglas, E., Dolan, C., Hamilton, H. (2011). “Small beam bond test method for CFRP composites applied to concrete.” *J.of Compos. Constr.,* 10(6), 52-61.

International Code Council (ICC). (2012). “AC125: Acceptance criteria for concrete and reinforced and unreinforced masonry strengthening using externally bonded FRP composite systems.” *ICC Evaluation Service,* Whittier, CA.

Jaipuriar, A., Flood, J., Bakis, C., Lopez, M., He, X. (2011). “Glassy-rubbery transition behavior of epoxy resins used in FRP structural strengthening systems.” *5th International Conference on FRP Composites in Civil Engineering (CICE), Beijing, China.*

Kim, W. S., Yun, I. H., Lee, J. J., Jung, H. T. (2010). “Evaluation of mechanical interlock effect on adhesion strength of polymer–metal interfaces using micro-patterned surface topography.” *Int. J. Adhes.* 30(6), 408-417.

Lu, M. G., Shim, M. J., Kim, S. W. (2001). “Effects of moisture on properties of epoxy molding compounds.” *J. Appl. Polym. Sci*., 81(9), 2253-2259

Moussa, O., Vassilopoulos, A. P., Castro, D., Keller, T. (2011). “Mechanical recovery of epoxy adhesive subsequent to exceeding glass transition temperature.” *4th International Conference on Durability of Composites for Construction (CDCC),* Quebec, Canada.

Nunez, L., Villanueva, M., Fraga, F., Nunez, M. R. (1999). “Influence of water absorption on the mechanical properties of a DGEBA epoxy system.” *J. Appl. Polym. Sci.,* 74(2), 353-358.

Osborne, L. (2013) “United States’ Rainiest Cities.” *National Climatic Data Center,* Asheville, NC.

Qiao, P. and Chen, Y. (2008) “Cohesive fracture simulation and failures modes of FRP-concrete bonded interfaces.” *J. of Theoretical and Applied Fracture Mechanics*, 49(2), 213-225.

Stewart, A. (2012). “Study of cement-epoxy interfaces, accelerated testing, and surface modification.” PhD Dissertation, Uni. of Florida, Gainesville, FL.

Tatar, J., Weston, C., Blackburn, P., Hamilton, H. (2013). “Direct shear adhesive bond test.” *11th International Symposium on Fiber Reinforced Polymers For Reinforced Concrete Structures,* Guimarães, Portugal.

Wunderlich, B. (2005) “Thermal analysis of polymeric materials.” *Springer*, The Netherlands.

Zhou, J. M. and Lucas, J. P. (1999). “Hygrothermal effects of epoxy resin. Part I: The nature of water in epoxy. Part II: Variations of glass transition temperature.” *Polymer, 40* (20), 5505-5522.

BIOGRAPHICAL SKETCH

Bethany “Paige” Blackburn was born to Margaret Brewster and Keith Blackburn in Anchorage, Alaska in 1990. In June of 2008, she moved from Alaska to Colorado and began attending the United States Air Force Academy. There she competed in division one track and field athletics and graduated with a bachelor’s degree in civil engineering in 2012. The Air Force granted her the opportunity to complete her master’s degree for her first assignment. In August of 2012, she traveled to the University of Florida to pursue a graduate degree in structural engineering under the direction of Dr. Trey Hamilton.